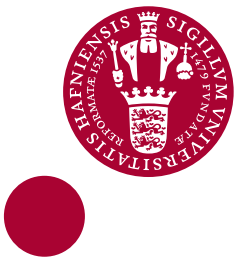

Pion and kaon condensation at zero temperature in three-flavor PT at nonzero isospin and strange chemical potentials at next-to-leading order

Adhikari, Prabal; Andersen, Jens O

Published in:
Journal of High Energy Physics (Online)

DOI:
10.1007/JHEP06(2020)170

Publication date:
2020

Document version
Publisher's PDF, also known as Version of record

JHEP

Published for SISSA by Springer

Received: March 1, 2020
Revised: May 16, 2020
Accepted: May 20, 2020
Published: June 26, 2020

Pion and kaon condensation at zero temperature in three-flavor χPT at nonzero isospin and strange chemical potentials at next-to-leading order

Prabal Adhikari[a,b,1] **and Jens O. Andersen**[b,c]

[a] *Wellesley College, Department of Physics, 106 Central Street, Wellesley, MA 02481, U.S.A.*
[b] *Department of Physics, Faculty of Natural Sciences, NTNU, Norwegian University of Science and Technology, Høgskoleringen 5, N-7491 Trondheim, Norway*
[c] *Niels Bohr International Academy, Blegdamsvej 17, DK-2100 Copenhagen, Denmark*

E-mail: pa100@wellesley.edu, andersen@tf.phys.ntnu.no

Abstract: We consider three-flavor chiral perturbation theory (χPT) at zero temperature and nonzero isospin (μ_I) and strange (μ_S) chemical potentials. The effective potential is calculated to next-to-leading order (NLO) in the $\pi^{\pm}$-condensed phase, the $K^{\pm}$-condensed phase, and the $K^0/\bar{K}^0$-condensed phase. It is shown that the transitions from the vacuum phase to these phases are second order and take place when, $|\mu_I| = m_\pi$, $|\frac{1}{2}\mu_I + \mu_S| = m_K$, and $|-\frac{1}{2}\mu_I + \mu_S| = m_K$, respectively at tree level and remains unchanged at NLO. The transition between the two condensed phases is first order. The effective potential in the pion-condensed phase is independent of μ_S and in the kaon-condensed phases, it only depends on the combinations $\pm\frac{1}{2}\mu_I + \mu_S$ and not separately on μ_I and μ_S. We calculate the pressure, isospin density and the equation of state in the pion-condensed phase and compare our results with recent $(2+1)$-flavor lattice QCD data. We find that the three-flavor χPT results are in good agreement with lattice QCD for $\mu_I < 200\,\text{MeV}$, however for larger values χPT produces values for observables that are consistently above lattice results. For $\mu_I > 200\,\text{MeV}$, the two-flavor results are in better agreement with lattice data. Finally, we consider the observables in the limit of very heavy s-quark, where they reduce to their two-flavor counterparts with renormalized couplings. The disagreement between the predictions of two and three flavor χPT can largely be explained by the differences in the experimental values of the low-energy constants.

Keywords: Chiral Lagrangians, Lattice QCD, Phase Diagram of QCD

ArXiv ePrint: 1909.10575

[1] Corresponding author.

https://doi.org/10.1007/JHEP06(2020)170

JHEP06(2020)170

Contents

1 Introduction **1**

2 χPT Lagrangian at $\mathcal{O}(p^4)$ **3**
2.1 Next-to-leading order Lagrangian 4

3 Ground state and fluctuations **5**
3.1 Parametrizing fluctuations 9
3.2 Leading-order Lagrangian 10
3.2.1 Normal phase 11
3.2.2 Pion-condensed phase 12
3.2.3 Charged kaon-condensed phase 13

4 Next-to-leading order effective potential **16**
4.1 Normal phase 16
4.2 Pion-condensed phase 17
4.3 Charged kaon-condensed phase 19

5 Thermodynamic functions **22**
5.1 Pion-condensed phase 22
5.2 Large-m_s limit 23

6 Results and discussion **25**
6.1 Phase diagram 27
6.2 Medium-dependent masses 28
6.3 Pressure, isospin density, and equation of state 30

A Meson masses and decay constants **33**

JHEP06(2020)170

1 Introduction

Quantum chromodynamics (QCD), the theory of the strong force, is challenging to study due to its non-perturbative nature and the inability to use lattice QCD simulations in the phenomenologically most interesting regime, namely finite baryon density, due to the infamous fermion sign problem [1, 2] present in classical Monte Carlo algorithms. As such, except for asymptotically large baryon chemical potentials, where QCD is expected to be in a color-flavor-locked phase [3, 4] and can be studied due to asymptotic freedom, most of the phenomenologically relevant QCD phase diagram must be mapped out by other methods, e.g. low-energy effective models.

Recently, there has been renewed interest in a slightly different regime of QCD, one with a finite isospin chemical potential due to the possibility of a new form of compact stars known as pion stars, first discussed in ref. [5]. This type of compact object could form in regions with large densities of neutrinos, which in turn leads to the production of pions and their subsequent condensation [6]. These pions under weak equilibrium lead to stable pion stars, which may be electromagnetically neutralized by either electrons or muons, or both. They are expected to have radii and masses that are substantially larger than those of neutron stars [7]. Pion stars are also different from neutron stars in the sense that at $T = 0$ it is interactions that give rise to an (effective) equation of state, and not the statistics of its constituents.

QCD at finite isospin chemical potential was first studied by Son and Stephanov using chiral perturbation theory (χPT) [8–12] in their seminal paper [13]. In refs. [5, 14–19] one can find various applications of χPT including some partial next-to-leading order results. Since then finite isospin systems have been studied extensively in other versions of QCD including two-color and adjoint QCD [20, 21], in the NJL [22–34], in the quark-meson model [35–38], but also through lattice QCD, where it does not suffer from the fermion sign problem (except at finite magnetic fields [39, 40] due to the charge asymmetry of the up and down quarks). The first lattice QCD calculations of finite isospin QCD were done in refs. [41, 42] and a more recent, thorough analysis in refs. [43–45]. They find as expected from chiral perturbation theory calculations that at zero temperature there is a second order phase transition at an isospin chemical potential, $|\mu_I| = m_\pi$,[1] which remains largely unaltered at finite temperatures up to approximately 170 MeV beyond which quarks become deconfined [15]. Similarly, with increasing isospin chemical potentials the quarks in the pions become more loosely bound and occur in a BCS phase though owing to the fact that this phase has the same order parameter as the BEC phase, there is no real phase transition, only a crossover transition, with the size of the pion condensate decreasing substantially within a narrow isospin window.

There have been a number of studies in recent years comparing $(2 + 1)$ flavor lattice QCD results with both QCD models and effective theories. Recently, the NJL model (non-renormalizable) comparisons [33] were made that showed good agreement with the lattice while the quark-meson model [38] (which is renormalizable) largely agrees with the lattice. Furthermore, there have been other comparisons of lattice QCD with results from an effective field theory (and model-independent) description [18], which is valid for asymptotically large isospin chemical potentials [16], where the pions behave as a free Bose gas. A recent review can be found in ref. [46].

The focus of this work is to compare the results of three-flavor χPT at finite isospin density [47] with that of $(2 + 1)$-flavor lattice QCD of refs. [43–45]. We previously studied two-flavor χPT at next-to-leading order (NLO) [48] and found that the NLO results are in better agreement with lattice QCD than the tree-level results though the pressure, isospin density and energy density were all found to be consistently smaller than lattice QCD values. This is not entirely unexpected since the lattice QCD observables included the

[1]The $|\mu_I| = \frac{1}{2}m_\pi$ conventions is also frequently found in the literature. See eq. (2.9).

JHEP06(2020)170

effects of the sea strange quarks [49] while two-flavor χPT does not. As such, we extend our previous work in NLO two-flavor χPT to include the effect of the strange quarks by using three-flavor χPT at finite isospin chemical potential and find that the observables near the second phase transition is in good agreement with lattice QCD. As a natural extension of our finite isospin study, we also construct the NLO, one-loop effective potential to study the effects of the simultaneous presence of both the isospin and strange quark chemical potential.[2] We find the second-order phase transition in the pion condensed phase remains at $|\mu_I| = m_\pi$ even with the inclusion of μ_S and NLO corrections.[3] Similarly, the second order phase transition in the kaon condensed phases remains at $|\pm\frac{1}{2}\mu_I + \mu_S| = m_K$ where m_K is the kaon mass. Furthermore the effective potential even in the presence of μ_S in the pion condensed phase only depends on μ_I and in the kaon condensed phases on the combination $\left|\pm\frac{1}{2}\mu_I + \mu_S\right|$ but not μ_I and μ_S separately.

The paper is organized as follows. In the next section, we discuss the Lagrangian of three-flavor chiral perturbation theory at finite isospin and strange chemical potentials at next-to-leading order in the low-energy expansion. In section 3, we review the ground state of the theory and fluctuations in the different phases. In section 4 the NLO effective potential in the three different phases of the theory is calculated. In section 5, we derive the pressure, isospin density, and equation of state in the pion-condensed phase. We also consider the large-m_s limit, where it is shown that the observables in three-flavor χPT reduce to the two-flavor observables of ref. [48] with renormalized couplings. In section 6, we discuss the phase diagram in more detail and derive medium-dependent masses at tree level. We compare our results for the thermodynamic functions with recent lattice simulations.

2 χPT Lagrangian at $\mathcal{O}(p^4)$

In this section, we briefly discuss the symmetries of three-flavor QCD as well the chiral Lagrangian to next-to-leading order in the low-energy expansion and its renormalization. The three-flavor Lagrangian of QCD is

$$\mathcal{L} = \bar{\psi}\left(i\not{D} - m\right)\psi - \frac{1}{4}F^a_{\mu\nu}F^{\mu\nu a}\,, \tag{2.1}$$

where $m = \mathrm{diag}(m_u, m_d, m_s)$ is the quark mass matrix, $\not{D} = \gamma^\mu\partial_\mu - ig\lambda^a A^a_\mu$ is the covariant derivative, λ^a are the Gell-Mann matrices, g is the strong coupling, A^a_μ is the gauge field, and $F^a_{\mu\nu}$ is the field-strength tensor. The global symmetry of massless three-flavor QCD is $\mathrm{SU}(3)_L \times \mathrm{SU}(3)_R \times \mathrm{U}(1)_B$, which is spontaneously broken down to $\mathrm{SU}(3)_V \times \mathrm{U}(1)_B$ in the vacuum. For two degenerate light quarks, i.e. in the isospin limit the symmetry is $\mathrm{SU}(2)_I \times \mathrm{U}(1)_Y \times \mathrm{U}(1)_B$, where Y represents hypercharge. If $m_u \neq m_d$, this symmetry is reduced to $\mathrm{U}(1)_{I_3} \times \mathrm{U}(1)_Y \times \mathrm{U}(1)_B$. If we add a chemical potential for each of the quarks, the symmetry is $\mathrm{U}(1)_{I_3} \times \mathrm{U}(1)_Y \times \mathrm{U}(1)_B$, irrespective of the quark masses.

In the present paper, we consider three-flavor QCD with two degenerate light quarks. The chiral Lagrangian then describes the octet of pseudo-Goldstone bosons consisting of

[2] Note that the "strange quark chemical potential" (μ_s) is different from the "strange chemical potential" (μ_S). We define them in eq. (2.10).

[3] This property is expected to hold to all orders in perturbation theory.

JHEP06(2020)170

the three pions ($\pi^{\pm}$ and π^0), the four kaons ($K^{\pm}$, K^0 and $\bar{K}^0$), and the eta (η). We begin with the chiral perturbation theory Lagrangian at $\mathcal{O}(p^2)$ [9][4]

$$\mathcal{L}_2 = \frac{f^2}{4}\mathrm{Tr}\left[\nabla_\mu \Sigma^\dagger \nabla^\mu \Sigma\right] + \frac{f^2}{4}\mathrm{Tr}\left[\chi^\dagger \Sigma + \chi \Sigma^\dagger\right] , \tag{2.2}$$

where f is the bare pion decay constant, $\chi = 2B_0 M$, and

$$M = \mathrm{diag}(m_u, m_d, m_s) \tag{2.3}$$

is the quark mass matrix, $\Sigma = U\Sigma_0 U$, where $U = \exp\frac{i\lambda_i\phi_i}{2f}$, and $\Sigma = \mathbb{1}$ is the vacuum. Moreover, λ_i $(i = 1, 2, \ldots, 8)$ are the Gell-Mann matrices that satisfy $\mathrm{Tr}\lambda_i\lambda_j = 2\delta_{ij}$ and ϕ_i are the fields that parametrize the Goldstone manifold. The covariant derivative at nonzero quark chemical μ_q potentials $(q = u, d, s)$ is defined as follows

$$\nabla_\mu \Sigma \equiv \partial_\mu \Sigma - i\left[v_\mu, \Sigma\right] , \tag{2.4}$$

$$\nabla_\mu \Sigma^\dagger = \partial_\mu \Sigma^\dagger - i[v_\mu, \Sigma^\dagger] , \tag{2.5}$$

where

$$v_\mu = \delta_{\mu 0}\mathrm{diag}(\mu_u, \mu_d, \mu_s) , \tag{2.6}$$

We can also express v_μ in terms of the baryon, isospin and strangeness chemical potentials μ_B, μ_I, and μ_S as

$$v_\mu = \delta_{\mu 0}\mathrm{diag}\left(\frac{1}{3}\mu_B + \frac{1}{2}\mu_I, \frac{1}{3}\mu_B - \frac{1}{2}\mu_I, \frac{1}{3}\mu_B - \mu_S\right) . \tag{2.7}$$

where

$$\mu_B = \frac{3}{2}(\mu_u + \mu_d) , \tag{2.8}$$

$$\mu_I = \mu_u - \mu_d , \tag{2.9}$$

$$\mu_S = \frac{1}{2}(\mu_u + \mu_d - 2\mu_s) . \tag{2.10}$$

This yields

$$v_0 = \frac{1}{3}(\mu_B - \mu_S)\mathbb{1} + \frac{1}{2}\mu_I\lambda_3 + \frac{1}{\sqrt{3}}\mu_S\lambda_8 . \tag{2.11}$$

We note that the μ_B-dependent term in eq. (2.11) commutes with Σ and $\Sigma^\dagger$ in eqs. (2.4)–(2.5) and so the baryon chemical potential drops completely out of the chiral Lagrangian. This reflects the fact that we have only included the mesonic octet, which has zero baryonic charge. We therefore set $\mu_B = 0$ in the remainder of the paper.

2.1 Next-to-leading order Lagrangian

In order to perform calculations beyond tree level, we must go to next-to-leading order in the low-energy expansion and consider the terms that contribute to $\mathcal{L}$ at $\mathcal{O}\left(p^4\right)$. There are

[4]One factor of ∇_μ counts one power of p and one factor of χ counts two powers of p.

JHEP06(2020)170

twelve operators in $\mathcal{L}_4$ [10], but only eight of them are relevant for the present calculations. They are

$$\begin{aligned}\mathcal{L}_4 = {} & L_1 \left(\mathrm{Tr}\left[\nabla_\mu \Sigma^\dagger \nabla^\mu \Sigma\right]\right)^2 + L_2 \mathrm{Tr}\left[\nabla_\mu \Sigma^\dagger \nabla_\nu \Sigma\right] \mathrm{Tr}\left[\nabla^\mu \Sigma^\dagger \nabla^\nu \Sigma\right] \\ & + L_3 \mathrm{Tr}\left[(\nabla_\mu \Sigma^\dagger \nabla^\mu \Sigma)(\nabla_\nu \Sigma^\dagger \nabla^\nu \Sigma)\right] + L_4 \mathrm{Tr}\left[\nabla_\mu \Sigma^\dagger \nabla^\mu \Sigma\right] \mathrm{Tr}\left[\chi^\dagger \Sigma + \chi \Sigma^\dagger\right] \\ & + L_5 \mathrm{Tr}\left[\left(\nabla_\mu \Sigma^\dagger \nabla^\mu \Sigma\right)\left(\chi^\dagger \Sigma + \chi \Sigma^\dagger\right)\right] + L_6 \left(\mathrm{Tr}\left[\chi^\dagger \Sigma + \chi \Sigma^\dagger\right]\right)^2 \\ & + L_8 \mathrm{Tr}\left[\chi^\dagger \Sigma \chi^\dagger \Sigma + \chi \Sigma^\dagger \chi \Sigma^\dagger\right] + H_2 \mathrm{Tr}\left[\chi^\dagger \chi\right] . \end{aligned} \tag{2.12}$$

where L_i and H_i are unrenormalized couplings. The relations between the bare and renormalized couplings $L_i^r(\Lambda)$ and $H_i^r(\Lambda)$ are

$$L_i = L_i^r(\Lambda) + \Gamma_i \lambda \,, \tag{2.13}$$

$$H_i = H_i^r(\Lambda) + \Delta_i \lambda \,, \tag{2.14}$$

where

$$\lambda = -\frac{\Lambda^{-2\epsilon}}{2(4\pi)^2}\left[\frac{1}{\epsilon} + 1\right] . \tag{2.15}$$

Here Γ_i and Δ_i are constants and Λ is the renormalization scale in the modified minimal substraction scheme $\overline{\mathrm{MS}}$. The renormalized couplings satisfy the renormalization group equations

$$\Lambda \frac{d}{d\Lambda} L_i^r = -\frac{\Gamma_i}{(4\pi)^2} \,, \qquad \Lambda \frac{d}{d\Lambda} H_i^r = -\frac{\Delta_i}{(4\pi)^2} \,. \tag{2.16}$$

These are obtained by differentiation of eqs. (2.13)–(2.14) noting that the bare parameters are independent of the scale Λ. The solutions are

$$L_i^r(\Lambda) = L_i^r(\Lambda_0) - \frac{\Gamma_i}{2(4\pi)^2} \log \frac{\Lambda^2}{\Lambda_0^2} \,, \qquad H_i^r(\Lambda) = H_i^r(\Lambda_0) - \frac{\Delta_i}{2(4\pi)^2} \log \frac{\Lambda^2}{\Lambda_0^2} \,, \tag{2.17}$$

where Λ_0 is a reference scale. We note that the contact term $H_2 \mathrm{Tr}[\chi^\dagger \chi]$ gives a constant contribution to the effective potential which is the same in all phases. We keep it, however, since it is needed to show the scale independence of the final result for the effective potential.

In three-flavor QCD, the constants Γ_i and Δ_i are

$$\Gamma_1 = \frac{3}{32} \,, \qquad \Gamma_2 = \frac{3}{16} \,, \qquad \Gamma_3 = 0 \,, \qquad \Gamma_4 = \frac{1}{8} \,, \tag{2.18}$$

$$\Gamma_5 = \frac{3}{8} \,, \qquad \Gamma_6 = \frac{11}{144} \,, \qquad \Gamma_8 = \frac{5}{48} \,, \qquad \Delta_2 = \frac{5}{24} \,. \tag{2.19}$$

3 Ground state and fluctuations

In this section, we will discuss the phase structure of the theory as a function of the chemical potentials μ_I and μ_S. We will also discuss how to parametrize the fluctuations above the ground state.

The most general SU(3) matrix for the ground state can be written as

$$\Sigma_\alpha = e^{i\alpha \hat{\phi}_i \lambda_i} \,, \tag{3.1}$$

JHEP06(2020)170

where α is a rotation angle, $\hat{\phi}_i$ are variational parameters and a sum over the repeated index i is implied. In order to ensure the normalization of the ground state, $\Sigma_\alpha \Sigma_\alpha^\dagger = \mathbb{1}$, the coefficients must satisfy $\sum_i \hat{\phi}_i^2 = 1$. However, depending on the chemical potentials, we expect that the ground state takes a certain form, i.e. that it is rotated in a specific way. For example, in the case $\mu_S = 0$, we expect pion condensation for $|\mu_I| > m_\pi$ [13] and that the two-flavor results carry over. We therefore briefly review the two-flavor case first. Here the ground state can be written as [13]

$$\Sigma_\alpha = e^{i\alpha\hat{\phi}_i\tau_i} = \cos\alpha + i\hat{\phi}_i\tau_i \sin\alpha\,, \tag{3.2}$$

where τ_i are the Pauli matrices and $\hat{\phi}_i$ are again variational parameters. The static part of the $\mathcal{O}(p^2)$ Hamiltonian $\mathcal{H}_2$ reads

$$\mathcal{H}_2^{\text{static}} = \frac{f^2}{4}\text{Tr}[v_0, \Sigma_\alpha][v_0, \Sigma_\alpha^\dagger] - \frac{f^2}{2}B_0\text{Tr}[M\Sigma_\alpha + M\Sigma_\alpha^\dagger]\,, \tag{3.3}$$

where in the two-flavor case $v_0 = \frac{1}{2}\tau_3\mu_I$, cf. eq. (2.11) and $M = \text{diag}(m_u, m_d) = \text{diag}(m, m)$. The first term in eq. (3.3) can be written as

$$\mathcal{H}_2^{\text{static (a)}} = \frac{f^2}{4}\text{Tr}[v_0, \Sigma_\alpha][v_0, \Sigma_\alpha^\dagger] = \frac{f^2}{8}\mu_I^2\text{Tr}[\tau_3\Sigma_\alpha\tau_3\Sigma_\alpha^\dagger - \mathbb{1}]\,. \tag{3.4}$$

This form suggests that $\mathcal{H}_2^{\text{static (a)}}$ favors directions that anticommute with τ_3 [13]. Substituting eq. (3.2) into eq. (3.4), this expectation is made explicit, $\mathcal{H}_2^{\text{static (a)}} = -\frac{1}{2}f^2\mu_I^2\sin^2\alpha(\hat{\phi}_1^2 + \hat{\phi}_2^2)$. Evaluating the other term in eq. (3.3), we find

$$\mathcal{H}_2^{\text{static}} = -2f^2B_0m\cos\alpha - \frac{1}{2}f^2\mu_I^2\sin^2\alpha(\hat{\phi}_1^2 + \hat{\phi}_2^2)\,. \tag{3.5}$$

The first term favors $\alpha = 0$, i.e. the vacuum state $\Sigma_0 = \mathbb{1}$, and it is clear that there is competition between the two terms in eq. (3.5). We notice that the static energy only depends on $\hat{\phi}_1^2 + \hat{\phi}_2^2$, and it is minimized by setting $\hat{\phi}_3 = 0$. Without loss of generality and for later convenience, we can choose $\hat{\phi}_1 = 1$ and $\hat{\phi}_2 = 0$. The rotated vacuum eq. (3.2) can then be written as

$$\Sigma_\alpha = A_\alpha\Sigma_0A_\alpha\,, \tag{3.6}$$

where

$$A_\alpha = e^{i\frac{\alpha}{2}\tau_1} = \cos\frac{\alpha}{2} + i\tau_1\sin\frac{\alpha}{2}\,. \tag{3.7}$$

Minimizing eq. (3.5) with respect to α, we find two phases, $\alpha = 0$ for $2B_0m < \mu_I^2$ and $\cos\alpha = \frac{2B_0m}{\mu_I^2}$ for $2B_0m > \mu_I^2$. The first phase is the vacuum phase and the second phase consists of a condensate of charged pions.

In analogy with the two-flavor case, we expect that pion condensation in the three-flavor case can be captured by writing eq. (3.1) as[5]

$$\Sigma_\alpha^{\pi^\pm} = A_\alpha\Sigma_0A_\alpha\,, \tag{3.8}$$

[5] λ_1 plays the role of τ_1 and λ_2 that of τ_2. We are free to choose any linear combination of the two and we choose λ_2.

JHEP06(2020)170

where

$$A_\alpha = e^{i\frac{\alpha}{2}\lambda_2} = \frac{1+2\cos\frac{\alpha}{2}}{3}\mathbb{1} + i\lambda_2 \sin\frac{\alpha}{2} + \frac{\cos\frac{\alpha}{2}-1}{\sqrt{3}}\lambda_8\,. \tag{3.9}$$

The rotated ground state can also be conveniently written as

$$\Sigma_\alpha^{\pi^\pm} = \begin{pmatrix} \cos\alpha & \sin\alpha & 0 \\ -\sin\alpha & \cos\alpha & 0 \\ 0 & 0 & 1 \end{pmatrix}, \tag{3.10}$$

which shows that the rotation does not affect the s-quark. The symmetry breaking pattern in this case is

$$\mathrm{U}(1)_{I_3} \times \mathrm{U}(1)_Y \times \mathrm{U}(1)_B \to \mathrm{U}(1)_Y \times \mathrm{U}(1)_B\,. \tag{3.11}$$

Since $\mathrm{U}(1)_Q \not\subset \mathrm{U}(1)_Y \times \mathrm{U}(1)_B$, electric charge Q is also broken and the system is both a superfluid and a superconductor.

We next consider kaon condensation in three-flavor χPT. Depending on the values of μ_I and μ_S, either the charged kaons or neutral kaons condense. If $|\frac{1}{2}\mu_I + \mu_S| = |\mu_u - \mu_s| > m_K$, we expect either K^+ or K^- to condense depending on the sign. If $|-\frac{1}{2}\mu_I + \mu_S| = |\mu_d - \mu_s| > m_K$, we expect K^0 or $\bar{K}^0$ to condense depending on the sign. In the case of charged kaon condensation, λ_4 and λ_5 replace λ_1 and λ_2, respectively, and without loss of generality we can write $\Sigma_\alpha^{K^\pm} = e^{i\frac{\alpha}{2}\lambda_5}\Sigma_0 e^{i\frac{\alpha}{2}\lambda_5}$. The rotated ground state takes the form

$$\begin{aligned} \Sigma_\alpha^{K^\pm} &= \frac{1+2\cos\alpha}{3}\mathbb{1} + \frac{\cos\alpha - 1}{2\sqrt{3}}\left(\sqrt{3}\lambda_3 - \lambda_8\right) + i\lambda_5\sin\alpha \\ &= \begin{pmatrix} \cos\alpha & 0 & \sin\alpha \\ 0 & 1 & 0 \\ -\sin\alpha & 0 & \cos\alpha \end{pmatrix}. \end{aligned} \tag{3.12}$$

The symmetry-breaking pattern is

$$\mathrm{U}(1)_{I_3} \times \mathrm{U}(1)_Y \times \mathrm{U}(1)_B \to \mathrm{U}(1)_Y \times \mathrm{U}(1)_B\,. \tag{3.13}$$

Again, since the $\mathrm{U}(1)_Q \not\subset \mathrm{U}(1)_Y \times \mathrm{U}(1)_B$, electric charge is spontaneously broken and the superfluid is also a superconductor.

Finally, in the case of neutral kaon condensation the rotated ground state is $\Sigma_\alpha^{K^0/\bar{K}^0} = e^{i\frac{\alpha}{2}\lambda_7}\Sigma_0 e^{i\frac{\alpha}{2}\lambda_7}$, or

$$\begin{aligned} \Sigma_\alpha^{K^0/\bar{K}^0} &= \frac{1+2\cos\alpha}{3}\mathbb{1} + \frac{1-\cos\alpha}{2\sqrt{3}}\left(\sqrt{3}\lambda_3 + \lambda_8\right) + i\lambda_7\sin\alpha \\ &= \begin{pmatrix} 1 & 0 & 0 \\ 0 & \cos\alpha & \sin\alpha \\ 0 & -\sin\alpha & \cos\alpha \end{pmatrix}. \end{aligned} \tag{3.14}$$

The symmetry-breaking pattern is now

$$\mathrm{U}(1)_{I_3} \times \mathrm{U}(1)_Y \times \mathrm{U}(1)_B \to \mathrm{U}(1)_Q \times \mathrm{U}(1)_B\,, \tag{3.15}$$

implying that the superfluid is not a superconductor.

JHEP06(2020)170

While we have considered the possibility of a single species condensing, in principle it is possible for the ground state to have simultaneous condensation of multiple mesons. However, explicit calculations in refs. [46, 47] that include the possibility of multiple rotations into multiple condensed phases show that such phases are not the global minima except on the first order transition line. We discuss the line at the end of this section.

We now return to the evaluation of the static Hamiltonian $\mathcal{H}_2$. In the case of pion condensation, the static Hamiltonian reduces to

$$\mathcal{H}_2 = -2f^2 B_0 m \cos\alpha - f^2 B_0 m_s - \frac{1}{2} f^2 \mu_I^2 \sin^2\alpha \,. \tag{3.16}$$

The minimum of the static Hamiltonian is

$$\cos\alpha = 1\,, \qquad \mu_I^2 < 2B_0 m \tag{3.17}$$

$$\cos\alpha = \frac{2B_0 m}{\mu_I^2}\,, \qquad \mu_I^2 > 2B_0 m\,. \tag{3.18}$$

The ground-state energy in the vacuum and pion-condensed phase is

$$\mathcal{H}_2 = -f^2 B_0 (2m + m_s)\,, \qquad \mu_I^2 < 2B_0 m\,, \tag{3.19}$$

$$\mathcal{H}_2 = -\frac{(2fB_0 m)^2}{\mu_I^2} - f^2 B_0 m_s - \frac{1}{2} f^2 \mu_I^2 \left(1 - \frac{(2B_0 m)^2}{\mu_I^4}\right)\,, \qquad \mu_I^2 > 2B_0 m\,. \tag{3.20}$$

In the case of charged kaon condensation, the static Hamiltonian reduces to

$$\mathcal{H}_2 = -f^2 B_0 m(1 + \cos\alpha) - f^2 B_0 m_s \cos\alpha - \frac{1}{2} f^2 \left(\frac{1}{2}\mu_I + \mu_S\right)^2 \sin^2\alpha\,. \tag{3.21}$$

The minimum of the static Hamiltonian is

$$\cos\alpha = 1\,, \qquad \left(\frac{1}{2}\mu_I + \mu_S\right)^2 < B_0(m + m_s) \tag{3.22}$$

$$\cos\alpha = \frac{B_0(m + m_s)}{(\frac{1}{2}\mu_I + \mu_S)^2}\,, \qquad \left(\frac{1}{2}\mu_I + \mu_S\right)^2 > B_0(m + m_s)\,. \tag{3.23}$$

The ground-state energy in the vacuum and the charged kaon-condensed phase is

$$\mathcal{H}_2 = -f^2 B_0 (2m + m_s)\,, \qquad \left(\frac{1}{2}\mu_I + \mu_S\right)^2 < B_0(m + m_s)\,, \tag{3.24}$$

$$\mathcal{H}_2 = -f^2 B_0 m - \frac{f^2 B_0^2 (m + m_s)^2}{(\frac{1}{2}\mu_I + \mu_S)^2} - \frac{1}{2} f^2 \left(\frac{1}{2}\mu_I + \mu_S\right)^2 \left(1 - \frac{B_0^2 (m + m_s)^2}{(\frac{1}{2}\mu_I + \mu_S)^4}\right)\,,$$

$$\left(\frac{1}{2}\mu_I + \mu_S\right)^2 > B_0(m + m_s)\,. \tag{3.25}$$

Finally, we consider the case of condensation of neutral kaons. The results for this phase can be obtained from the results of the phase of condensed charged kaons by the substitution $\mu_I \to -\mu_I$ since $-\frac{1}{2}\mu_I + \mu_S = \mu_d - \mu_s$. In order to find the global minimum, we must compare eqs. (3.20) and (3.25) in the region $|\mu_I| > m_\pi$ and $|\frac{1}{2}\mu_I + \mu_S| > m_K$. The boundary

JHEP06(2020)170

between the pion-condensed phase and the kaon-condensed phase is then given by equating these expressions. This yields

$$-\frac{\left(\mu_I^2 - m_\pi^2\right)^2}{2\mu_I^2} = -\frac{\left[m_K^2 - (\frac{1}{2}\mu_I + \mu_S)^2\right]^2}{2(\frac{1}{2}\mu_I + \mu_S)^2}\,, \tag{3.26}$$

or

$$\left|\pm\frac{1}{2}\mu_I + \mu_S\right| = \frac{\mu_I^2 - m_\pi^2 + \sqrt{(\mu_I^2 - m_\pi^2)^2 + 4\mu_I^2 m_K^2}}{2\mu_I}\,, \tag{3.27}$$

where we used the tree-level relations $m_\pi^2 = 2B_0 m$ and $m_K^2 = B_0(m + m_s)$. We will return to the phase diagram in the μ_I–μ_S plane in section 6.1.

3.1 Parametrizing fluctuations

Since we want to study the thermodynamics of the pion-condensed and kaon-condensed phases including leading-order quantum corrections, it is natural to expand the chiral perturbation theory Lagrangian around the relevant ground state. The Goldstone manifold as a consequence of chiral symmetry breaking is $\mathrm{SU}(3)_L \times \mathrm{SU}(3)_R/\mathrm{SU}(3)_V$. We will focus on the pion-condensed phase for simplicity. The remarks below also apply to the kaon-condensed phases. Following refs. [21, 48], we write

$$\Sigma = L_\alpha \Sigma_\alpha R_\alpha^\dagger\,, \tag{3.28}$$

with

$$L_\alpha = A_\alpha U A_\alpha^\dagger\,, \tag{3.29}$$

$$R_\alpha = A_\alpha^\dagger U^\dagger A_\alpha\,. \tag{3.30}$$

We emphasize that the fluctuations parameterized by L_α and R_α around the ground state depend on α since the broken generators (of QCD) need to be rotated appropriately as the condensed vacuum rotates with the angle α [21]. In the present case, U is an SU(3) matrix that parameterizes the fluctuations around the vacuum,

$$U = \exp\left(i\frac{\phi_a \lambda_a}{2f}\right)\,. \tag{3.31}$$

With the parameterizations stated above, we get

$$\Sigma = A_\alpha (U\Sigma_0 U) A_\alpha\,. \tag{3.32}$$

This parameterization not only produces the correct linear terms that vanish when evaluated at the minimum of the static Hamiltonian $\mathcal{O}(p^2)$, the divergences of the one-loop vacuum diagrams also cancel using counterterms from the $\mathcal{O}(p^4)$ Lagrangian. Furthermore, the parametrization produces a Lagrangian that is canonical in the fluctuations and has the correct limit when $\alpha = 0$, whereby

$$\Sigma = U\Sigma_0 U = U^2 = \exp\left(i\frac{\phi_a \lambda_a}{f}\right)\,, \tag{3.33}$$

JHEP06(2020)170

as expected. If one expands the Lagrangian using the parametrization $\Sigma = L\Sigma_\alpha R = U\Sigma_\alpha U = UA_\alpha\Sigma_0 A_\alpha U$ instead of eq. (3.28), the kinetic terms of the Lagrangian are non-canonical. By a field redefinition that depends on the chemical potentials, these terms can be made canonical. However, calculating the leading corrections to the tree-level potential, it can be shown that the ultraviolet divergences can be eliminated by renormalization only at the minimum of the classical potential.[6] Thus one cannot find the minimum of the next-to-leading order effective potential as a function of α, showing that this parametrization is erroneous. Let us finally take a look at the rotated generators. To linear order in the ϕ_i, an infinitesimal fluctuation can be written as

$$L_\alpha = \begin{pmatrix} \cos\frac{\alpha}{2} & \sin\frac{\alpha}{2} & 0 \\ -\sin\frac{\alpha}{2} & \cos\frac{\alpha}{2} & 0 \\ 0 & 0 & 1 \end{pmatrix} \left[1 + i\frac{\phi_i\lambda_i}{2f}\right] \begin{pmatrix} \cos\frac{\alpha}{2} & -\sin\frac{\alpha}{2} & 0 \\ \sin\frac{\alpha}{2} & \cos\frac{\alpha}{2} & 0 \\ 0 & 0 & 1 \end{pmatrix} . \tag{3.34}$$

Using the (anti)commutator relations of the Gell-Mann matrices, eq. (3.34) takes the form

$$\begin{aligned} L_\alpha = 1 &+ \frac{i\phi_1}{2f}(\cos\alpha\lambda_1 + \sin\alpha\lambda_3) + \frac{i\phi_2\lambda_2}{2f} + \frac{i\phi_3}{2f}(\cos\alpha\lambda_3 - \sin\alpha\lambda_1) \\ &+ \frac{i\phi_4}{2f}\left(\cos\frac{\alpha}{2}\lambda_4 - \sin\frac{\alpha}{2}\lambda_6\right) + \frac{i\phi_5}{2f}\left(\cos\frac{\alpha}{2}\lambda_5 - \sin\frac{\alpha}{2}\lambda_7\right) + \frac{i\phi_6}{2f}\left(\cos\frac{\alpha}{2}\lambda_6 + \sin\frac{\alpha}{2}\lambda_4\right) \\ &+ \frac{i\phi_7}{2f}\left(\cos\frac{\alpha}{2}\lambda_7 + \sin\frac{\alpha}{2}\lambda_5\right) + \frac{i\phi_8\lambda_8}{2f} . \end{aligned} \tag{3.35}$$

The linear combinations $\lambda_1' = (\cos\alpha\lambda_1 + \sin\alpha\lambda_3)$, $\lambda_2' = \lambda_2$, etc can be thought of as rotated generators, some of them, however, only by half the angle. The rotated generators λ_i' satisfy the same (anti)commutation relations as do λ_i To all orders in α, we then have

$$L_\alpha = \exp\left(\frac{i\phi_i\lambda_i'}{2f}\right) . \tag{3.36}$$

3.2 Leading-order Lagrangian

Using the parameterization eq. (3.32) discussed above, we can write down the Lagrangian in terms of the fields ϕ_a, which parametrizes the Goldstone manifold. The leading-order terms in the low-energy expansion are given by $\mathcal{L}_2$, which can be expanded as a power series in the fields

$$\mathcal{L}_2 = \mathcal{L}_2^{\text{linear}} + \mathcal{L}_2^{\text{static}} + \mathcal{L}_2^{\text{quadratic}} + \cdots \tag{3.37}$$

where the ellipses indicate terms that are cubic or higher order in the fields. We will carry out the expansion for the normal phase, the pion-condensed phase, and the charged kaon-condensed phase. Similar results can be obtained for the neutral kaon-condensed phase.

[6] Renormalization of the effective potential is carried out by renormalizing the low-energy constants in the NLO static Lagrangian, see section 4.

JHEP06(2020)170

3.2.1 Normal phase

In the normal phase, the different terms in eq. (3.37) are

$$\mathcal{L}_2^{\text{static}} = f^2 B_0(2m + m_s)\,, \tag{3.38}$$

$$\mathcal{L}_2^{\text{linear}} = 0\,, \tag{3.39}$$

$$\begin{aligned}\mathcal{L}_2^{\text{quadratic}} = {} & \frac{1}{2}\partial_\mu\phi_a\partial^\mu\phi^a - \frac{1}{2}\left(2B_0 m - \mu_I^2\right)\left(\phi_1^2 + \phi_2^2\right) - \frac{1}{2}(2B_0 m)\phi_3^2 \\ & - \frac{1}{2}\left[B_0(m + m_s) - \left(\frac{1}{2}\mu_I + \mu_S\right)^2\right]\left(\phi_4^2 + \phi_5^2 + \phi_6^2 + \phi_7^2\right) \\ & - \frac{B_0(m + 2m_s)}{3}\phi_8^2 + \mu_I(\phi_1\partial_0\phi_2 - \phi_2\partial_0\phi_1) + \left(\frac{1}{2}\mu_I + \mu_S\right)(\phi_4\partial_0\phi_5 - \phi_5\partial_0\phi_4) \\ & + \left(-\frac{1}{2}\mu_I + \mu_S\right)(\phi_6\partial_0\phi_7 - \phi_7\partial_0\phi_6)\,.\end{aligned} \tag{3.40}$$

The inverse propagator is block diagonal and can be written as

$$D^{-1} = \begin{pmatrix} D_{12}^{-1} & 0 & 0 & 0 & 0 \\ 0 & P^2 - m_3^2 & 0 & 0 & 0 \\ 0 & 0 & D_{45}^{-1} & 0 & 0 \\ 0 & 0 & 0 & D_{67}^{-1} & 0 \\ 0 & 0 & 0 & 0 & P^2 - m_8^2 \end{pmatrix}, \tag{3.41}$$

$$m_3^2 = 2B_0 m\,, \tag{3.42}$$

$$m_8^2 = \frac{2B_0(m + 2m_s)}{3}\,, \tag{3.43}$$

where $P = (p_0, p)$ is the four-momentum and $P^2 = p_0^2 - p^2$. The submatrices are

$$D_{12}^{-1} = \begin{pmatrix} P^2 - m_1^2 & ip_0 m_{12} \\ -ip_0 m_{12} & P^2 - m_2^2 \end{pmatrix}, \qquad D_{45}^{-1} = \begin{pmatrix} P^2 - m_4^2 & ip_0 m_{45} \\ -ip_0 m_{45} & P^2 - m_5^2 \end{pmatrix}, \tag{3.44}$$

$$D_{67}^{-1} = \begin{pmatrix} P^2 - m_6^2 & ip_0 m_{67} \\ -ip_0 m_{67} & P^2 - m_7^2 \end{pmatrix}, \tag{3.45}$$

The masses are

$$m_1^2 = 2B_0 m - \mu_I^2\,, \tag{3.46}$$

$$m_2^2 = m_1^2\,, \tag{3.47}$$

$$m_{12} = 2\mu_I\,, \tag{3.48}$$

$$m_4^2 = B_0(m + m_s) - \left(\frac{1}{2}\mu_I + \mu_S\right)^2, \tag{3.49}$$

$$m_5^2 = m_4^2\,, \tag{3.50}$$

$$m_{45} = \mu_I + 2\mu_S\,, \tag{3.51}$$

$$m_6^2 = m_4^2\,, \tag{3.52}$$

$$m_7^2 = m_4^2\,, \tag{3.53}$$

$$m_{67} = -\mu_I + 2\mu_S\,. \tag{3.54}$$

JHEP06(2020)170

The dispersion relations for the charges mesons are

$$E_{\pi^\pm} = \sqrt{p^2 + 2B_0 m} \pm \mu_I = \sqrt{p^2 + m_{\pi,0}^2} \pm \mu_I \,, \tag{3.55}$$

$$E_{\pi^0} = \sqrt{p^2 + 2B_0 m} = \sqrt{p^2 + m_{\pi,0}^2} \,, \tag{3.56}$$

$$E_{K^\pm} = \sqrt{p^2 + B_0(m+m_s)} \pm \left(\frac{1}{2}\mu_I + \mu_S\right) = \sqrt{p^2 + m_{K,0}^2} \pm \left(\frac{1}{2}\mu_I + \mu_S\right) \,, \tag{3.57}$$

$$E_{K^0} = \sqrt{p^2 + B_0(m+m_s)} \pm \left(-\frac{1}{2}\mu_I + \mu_S\right) = \sqrt{p^2 + m_{K,0}^2} \pm \left(-\frac{1}{2}\mu_I + \mu_S\right) \,, \tag{3.58}$$

$$E_\eta = \sqrt{p^2 + \frac{2}{3}B_0(m+2m_s)} = \sqrt{p^2 + m_{\eta,0}^2} \,. \tag{3.59}$$

The tree-level masses of the pions, kaons, and the η are then given by $m_{\pi,0}^2 = 2B_0 m$, $m_{K,0}^2 = B_0(m+m_s)$, and $m_{\eta,0}^2 = \frac{2}{3}B_0(m+2m_s)$.

3.2.2 Pion-condensed phase

In the pion-condensed phase, the different terms in eq. (3.37) are

$$\mathcal{L}_2^{\text{static}} = f^2 B_0(2m\cos\alpha + m_s) + \frac{1}{2}f^2\mu_I^2\sin^2\alpha \,, \tag{3.60}$$

$$\mathcal{L}_2^{\text{linear}} = f(-2B_0 m + \mu_I^2\cos\alpha)\sin\alpha\phi_2 - f\mu_I\sin\alpha\partial_0\phi_1 \,, \tag{3.61}$$

$$\begin{aligned}
\mathcal{L}_2^{\text{quadratic}} = {} & \frac{1}{2}\partial_\mu\phi_a\partial^\mu\phi_a - \frac{1}{2}\left(2B_0 m\cos\alpha - \mu_I^2\cos^2\alpha\right)\phi_1^2 \\
& - \frac{1}{2}\left(2B_0 m\cos\alpha - \mu_I^2\cos 2\alpha\right)\phi_2^2 - \frac{1}{2}\left(2B_0 m\cos\alpha + \mu_I^2\sin^2\alpha\right)\phi_3^2 \\
& - \frac{1}{2}\left[B_0(m\cos\alpha + m_s) - \frac{1}{4}\mu_I^2\cos 2\alpha - \mu_I\mu_S\cos\alpha - \mu_S^2\right](\phi_4^2 + \phi_5^2) \\
& - \frac{1}{2}\left[B_0(m\cos\alpha + m_s) - \frac{1}{4}\mu_I^2\cos 2\alpha + \mu_I\mu_S\cos\alpha - \mu_S^2\right](\phi_6^2 + \phi_7^2) \\
& - \frac{B_0(m\cos\alpha + 2m_s)}{3}\phi_8^2 + \mu_I\cos\alpha(\phi_1\partial_0\phi_2 - \phi_2\partial_0\phi_1) \\
& + \left(\frac{1}{2}\mu_I\cos\alpha + \mu_S\right)(\phi_4\partial_0\phi_5 - \phi_5\partial_0\phi_4) + \left(-\frac{1}{2}\mu_I\cos\alpha + \mu_S\right)(\phi_6\partial_0\phi_7 - \phi_7\partial_0\phi_6) \,.
\end{aligned} \tag{3.62}$$

We get for the inverse propagator:

$$D^{-1} = \begin{pmatrix} D_{12}^{-1} & 0 & 0 & 0 & 0 \\ 0 & p^2 - m_3^2 & 0 & 0 & 0 \\ 0 & 0 & D_{45}^{-1} & 0 & 0 \\ 0 & 0 & 0 & D_{67}^{-1} & 0 \\ 0 & 0 & 0 & 0 & P^2 - m_8^2 \end{pmatrix} , \tag{3.63}$$

$$m_3^2 = 2B_0 m\cos\alpha + \mu_I^2\sin^2\alpha \,, \tag{3.64}$$

$$m_8^2 = \frac{2B_0(m\cos\alpha + 2m_s)}{3} \,. \tag{3.65}$$

JHEP06(2020)170

The three different 2×2 matrices are given by

$$D_{12}^{-1} = \begin{pmatrix} P^2 - m_1^2 & ip_0 m_{12} \\ -ip_0 m_{12} & P^2 - m_2^2 \end{pmatrix}, \qquad D_{45}^{-1} = \begin{pmatrix} P^2 - m_4^2 & ip_0 m_{45} \\ -ip_0 m_{45} & P^2 - m_5^2 \end{pmatrix}, \tag{3.66}$$

$$D_{67}^{-1} = \begin{pmatrix} P^2 - m_6^2 & ip_0 m_{67} \\ -ip_0 m_{67} & P^2 - m_7^2 \end{pmatrix}, \tag{3.67}$$

where the masses are

$$m_1^2 = 2B_0 m \cos\alpha - \mu_I^2 \cos^2\alpha\,, \tag{3.68}$$

$$m_2^2 = 2B_0 m \cos\alpha - \mu_I^2 \cos 2\alpha\,, \tag{3.69}$$

$$m_{12} = 2\mu_I \cos\alpha\,, \tag{3.70}$$

$$m_4^2 = B_0(m\cos\alpha + m_s) - \frac{\mu_I^2}{4}\cos 2\alpha - \mu_I \mu_S \cos\alpha - \mu_S^2\,, \tag{3.71}$$

$$m_5^2 = m_4^2\,, \tag{3.72}$$

$$m_{45} = \mu_I \cos\alpha + 2\mu_S\,, \tag{3.73}$$

$$m_6^2 = B_0(m\cos\alpha + m_s) - \frac{\mu_I^2}{4}\cos 2\alpha + \mu_I \mu_S \cos\alpha - \mu_S^2\,, \tag{3.74}$$

$$m_7^2 = m_6^2\,, \tag{3.75}$$

$$m_{67} = -\mu_I \cos\alpha + 2\mu_S\,. \tag{3.76}$$

The quasiparticle dispersion relations can be easily found and read

$$E_{\pi^0} = p^2 + m_3^2\,, \tag{3.77}$$

$$E_{\pi^\pm}^2 = p^2 + \frac{1}{2}\left(m_1^2 + m_2^2 + m_{12}^2\right) \pm \frac{1}{2}\sqrt{4p^2 m_{12}^2 + (m_1^2 + m_2^2 + m_{12}^2)^2 - 4m_1^2 m_2^2}\,, \tag{3.78}$$

$$E_{K^\pm}^2 = p^2 + \frac{1}{2}\left(m_4^2 + m_5^2 + m_{45}^2\right) \pm \frac{1}{2}\sqrt{4p^2 m_{45}^2 + (m_4^2 + m_5^2 + m_{45}^2)^2 - 4m_4^2 m_5^2}\,, \tag{3.79}$$

$$E_{K^0}^2 = p^2 + \frac{1}{2}\left(m_6^2 + m_7^2 + m_{67}^2\right) \pm \frac{1}{2}\sqrt{4p^2 m_{67}^2 + (m_6^2 + m_7^2 + m_{67}^2)^2 - 4m_6^2 m_7^2}\,, \tag{3.80}$$

$$E_{\eta^0}^2 = p^2 + m_8^2\,. \tag{3.81}$$

3.2.3 Charged kaon-condensed phase

In the kaon-condensed phase, the different terms in eq. (3.37) are

$$\mathcal{L}_2^{\text{static}} = f^2 B_0[m + (m + m_s)\cos\alpha] + \frac{1}{2}f^2\left(\frac{1}{2}\mu_I + \mu_S\right)^2 \sin^2\alpha \tag{3.82}$$

$$\begin{aligned}\mathcal{L}_2^{\text{linear}} = {} & f\left[-B_0(m + m_s) + \left(\frac{1}{2}\mu_I + \mu_S\right)^2 \cos\alpha\right]\sin\alpha\phi_5 \\ & - f\left(\frac{1}{2}\mu_I + \mu_S\right)\sin\alpha\partial_0\phi_4\end{aligned} \tag{3.83}$$

$$\begin{aligned}\mathcal{L}_2^{\text{quadratic}} = {} & \frac{1}{2}\partial_\mu\phi_a\partial^\mu\phi_a - \frac{1}{2}\left\{\frac{1}{2}B_0\left[3m - m_s + (m + m_s)\cos\alpha\right]\right. \\ & \left. - \frac{1}{16}\left[3\mu_I - 2\mu_S + 2\left(\frac{1}{2}\mu_I + \mu_S\right)\cos\alpha\right]^2 + \frac{1}{4}\left(\frac{1}{2}\mu_I + \mu_S\right)^2 \sin^2\alpha\right\}(\phi_1^2 + \phi_2^2)\end{aligned}$$

JHEP06(2020)170

$$
\begin{aligned}
&-\frac{1}{2}\left\{\frac{1}{2}B_0\left[3m-m_s+(m+m_s)\cos\alpha\right]+\frac{1}{4}\left(\frac{1}{2}\mu_I+\mu_S\right)^2\sin^2\alpha\right\}\phi_3^2\\
&-\frac{1}{2}\left\{B_0(m+m_s)\cos\alpha-\left(\frac{1}{2}\mu_I+\mu_S\right)^2\cos^2\alpha\right\}\phi_4^2\\
&-\frac{1}{2}\left\{B_0(m+m_s)\cos\alpha-\left(\frac{1}{2}\mu_I+\mu_S\right)^2\cos 2\alpha\right\}\phi_5^2\\
&-\frac{1}{2}\left\{\frac{1}{2}B_0(m+m_s)(1+\cos\alpha)-\frac{1}{16}\left[-3\mu_I+2\mu_S+2\left(\frac{1}{2}\mu_I+\mu_S\right)\cos\alpha\right]^2\right.\\
&\qquad\left.+\frac{1}{4}\left(\frac{1}{2}\mu_I+\mu_S\right)^2\sin^2\alpha\right\}(\phi_6^2+\phi_7^2)\\
&-\frac{1}{2}\left\{\left[\frac{1}{6}B_0(-m+3m_s+5(m+m_s)\cos\alpha)+\frac{3}{4}\left(\frac{1}{2}\mu_I+\mu_S\right)^2\sin^2\alpha\right]\right\}\phi_8^2\\
&-\left\{\frac{1}{2\sqrt{3}}B_0(m+m_s)(\cos\alpha-1)+\frac{\sqrt{3}}{4}\left(\frac{1}{2}\mu_I+\mu_S\right)^2\sin^2\alpha\right\}\phi_3\phi_8\\
&+\frac{1}{4}\left[3\mu_I-2\mu_S+2\left(\frac{1}{2}\mu_I+\mu_S\right)\cos\alpha\right](\phi_1\partial_0\phi_2-\phi_2\partial_0\phi_1)\\
&+\left(\frac{1}{2}\mu_I+\mu_S\right)\cos\alpha(\phi_4\partial_0\phi_5-\phi_5\partial_0\phi_4)\\
&+\frac{1}{4}\left[-3\mu_I+2\mu_S+2\left(\frac{1}{2}\mu_I+\mu_S\right)\cos\alpha\right](\phi_6\partial_0\phi_7-\phi_7\partial_0\phi_6)\,. \qquad (3.84)
\end{aligned}
$$

The inverse propagator is block diagonal and can be written as

$$
D^{-1}=\begin{pmatrix} D_{12}^{-1} & 0 & 0 & 0\\ 0 & D_{38}^{-1} & 0 & 0\\ 0 & 0 & D_{45}^{-1} & 0\\ 0 & 0 & 0 & D_{67}^{-1}\end{pmatrix}, \qquad (3.85)
$$

where the submatrices are

$$
D_{12}^{-1}=\begin{pmatrix} P^2-m_1^2 & ip_0m_{12}\\ -ip_0m_{12} & P^2-m_2^2\end{pmatrix}, \qquad D_{38}^{-1}=\begin{pmatrix} P^2-m_3^2 & -m_{38}^2\\ -m_{38}^2 & P^2-m_8^2\end{pmatrix}, \qquad (3.86)
$$

$$
D_{45}^{-1}=\begin{pmatrix} P^2-m_4^2 & ip_0m_{45}\\ -ip_0m_{45} & P^2-m_5^2\end{pmatrix}, \qquad D_{67}^{-1}=\begin{pmatrix} P^2-m_6^2 & ip_0m_{67}\\ -ip_0m_{67} & P^2-m_7^2\end{pmatrix}. \qquad (3.87)
$$

JHEP06(2020)170

The masses are

$$m_1^2 = \left\{ \frac{1}{2} B_0 \left[3m - m_s + (m + m_s) \cos\alpha \right] \right.$$
$$\left. - \frac{1}{16} \left[3\mu_I - 2\mu_S + 2 \left(\frac{1}{2}\mu_I + \mu_S \right) \cos\alpha \right]^2 + \frac{1}{4} \left(\frac{1}{2}\mu_I + \mu_S \right)^2 \sin^2\alpha \right\}, \quad (3.88)$$

$$m_2^2 = m_1^2, \quad (3.89)$$

$$m_{12} = \frac{1}{2} \left[3\mu_I - 2\mu_S + 2 \left(\frac{1}{2}\mu_I + \mu_S \right) \cos\alpha \right], \quad (3.90)$$

$$m_3^2 = \left\{ \frac{1}{2} B_0 \left[3m - m_s + (m + m_s) \cos\alpha \right] + \frac{1}{4} \left(\frac{1}{2}\mu_I + \mu_S \right)^2 \sin^2\alpha \right\}, \quad (3.91)$$

$$m_4^2 = \left\{ B_0 (m + m_s) \cos\alpha - \left(\frac{1}{2}\mu_I + \mu_S \right)^2 \cos^2\alpha \right\}, \quad (3.92)$$

$$m_5^2 = \left\{ B_0 (m + m_s) \cos\alpha - \left(\frac{1}{2}\mu_I + \mu_S \right)^2 \cos 2\alpha \right\}, \quad (3.93)$$

$$m_{45} = 2 \left(\frac{1}{2}\mu_I + \mu_S \right) \cos\alpha, \quad (3.94)$$

$$m_6^2 = \left\{ \frac{1}{2} B_0 (m + m_s)(1 + \cos\alpha) - \frac{1}{16} \left[-3\mu_I + 2\mu_S + 2 \left(\frac{\mu_I}{2} + \mu_S \right) \cos\alpha \right]^2 \right.$$
$$\left. + \frac{1}{4} \left(\frac{1}{2}\mu_I + \mu_S \right)^2 \sin^2\alpha \right\}, \quad (3.95)$$

$$m_7^2 = m_6^2, \quad (3.96)$$

$$m_{67} = \frac{1}{2} \left[-3\mu_I + 2\mu_S + 2 \left(\frac{1}{2}\mu_I + \mu_S \right) \cos\alpha \right], \quad (3.97)$$

$$m_8^2 = \left[\frac{1}{6} B_0 (-m + 3m_s + 5(m + m_s) \cos\alpha) + \frac{3}{4} \left(\frac{1}{2}\mu_I + \mu_S \right)^2 \sin^2\alpha \right], \quad (3.98)$$

$$m_{38}^2 = \frac{1}{2\sqrt{3}} B_0 (m + m_s)(\cos\alpha - 1) + \frac{\sqrt{3}}{4} \left(\frac{1}{2}\mu_I + \mu_S \right)^2 \sin^2\alpha. \quad (3.99)$$

The quasiparticle dispersion relations can be easily found and read

$$E_{\pi^0}^2 = p^2 + \frac{1}{2}(m_3^2 + m_8^2) + \frac{1}{2}\sqrt{(m_3^2 - m_8^2)^2 + 4m_{38}^4}, \quad (3.100)$$

$$E_{\pi^\pm}^2 = p^2 + \frac{1}{2}\left(m_1^2 + m_2^2 + m_{12}^2\right) \pm \frac{1}{2}\sqrt{4p^2 m_{12}^2 + (m_1^2 + m_2^2 + m_{12}^2)^2 - 4m_1^2 m_2^2}, \quad (3.101)$$

$$E_{K^\pm}^2 = p^2 + \frac{1}{2}\left(m_4^2 + m_5^2 + m_{45}^2\right) \pm \frac{1}{2}\sqrt{4p^2 m_{45}^2 + (m_4^2 + m_5^2 + m_{45}^2)^2 - 4m_4^2 m_5^2}, \quad (3.102)$$

$$E_{K^0}^2 = p^2 + \frac{1}{2}\left(m_6^2 + m_7^2 + m_{67}^2\right) \pm \frac{1}{2}\sqrt{4p^2 m_{67}^2 + (m_6^2 + m_7^2 + m_{67}^2)^2 - 4m_6^2 m_7^2}, \quad (3.103)$$

$$E_{\eta^0}^2 = p^2 + \frac{1}{2}(m_3^2 + m_8^2) - \frac{1}{2}\sqrt{(m_3^2 - m_8^2)^2 + 4m_{38}^4}. \quad (3.104)$$

The linear terms in the condensed phases are given by eqs. (3.61) and (3.83). By differentiation with respect to α, it is straightforward to see that the terms vanish at the extremum

JHEP06(2020)170

of the corresponding static Lagrangian. To show this at NLO, requires the calculation of the one-loop diagram that contribute to the one-point function, see ref. [48] for details.

4 Next-to-leading order effective potential

In this section, we calculate the NLO effective potential in the three different phases we consider. At $\mathcal{O}(p^2)$, the contribution to the effective potential in each phase is given by evaluating $-\mathcal{L}_2^{\text{static}}$ using $\Sigma_\alpha^{\pi^\pm}$, $\Sigma_\alpha^{K^\pm}$, or $\Sigma_\alpha^{K^0/\bar{K}^0}$. At $\mathcal{O}(p^4)$, there are two contributions to the effective potential. The first is the Gaussian fluctuation about the ground state, i.e. the standard one-loop contribution. The second is given by evaluating $-\mathcal{L}_4^{\text{static}}$, again using $\Sigma_\alpha^{\pi^\pm}$, $\Sigma_\alpha^{K^\pm}$, or $\Sigma_\alpha^{K^0/\bar{K}^0}$. The one-loop contribution is ultraviolet divergent and needs regularization. We regularize the ultraviolet divergences using dimensional regularization in $d = 3 - 2\epsilon$ dimensions. The divergences are cancelled by renormalizing the coupling constants that multiply the operators in $\mathcal{L}_4$. The sum of the three contributions is the complete effective potential to $\mathcal{O}(p^4)$ in χPT.

After going to Euclidean space, the one-loop contribution to the effective potential of a free massive boson is given by

$$V_1 = \frac{1}{2}\int_P \log\left[P^2 + m^2\right] = \frac{1}{2}\int \frac{dp_0}{2\pi}\int_p \log\left[p_0^2 + p^2 + m^2\right] , \tag{4.1}$$

where m is the mass and the second integral is defined in $d = 3 - 2\epsilon$ as dimensions

$$\int_p = \left(\frac{e^{\gamma_E}\Lambda^2}{4\pi}\right)^\epsilon \int \frac{d^d p}{(2\pi)^d} , \tag{4.2}$$

and where Λ is the renormalization scale associated with the modified minimal subtraction scheme ($\overline{\text{MS}}$). Integrating over P_0, one finds

$$V_1 = \frac{1}{2}\int_p \sqrt{p^2 + m^2} = -\frac{m^4}{4(4\pi)^2}\left(\frac{\Lambda^2}{m^2}\right)^\epsilon \left[\frac{1}{\epsilon} + \frac{3}{2} + \mathcal{O}(\epsilon)\right] . \tag{4.3}$$

4.1 Normal phase

The leading-order contribution to the effective potential is minus the static Lagrangian given in eq. (3.38)

$$V_0 = -f^2 B_0(2m + m_s) . \tag{4.4}$$

The one-loop contribution to the effective potential is

$$V_1 = \frac{1}{2}\int_p \left[E_{\pi^+} + E_{\pi^-} + E_{\pi^0} + E_{K^+} + E_{K^-} + E_{K^0} + E_{\bar{K}^0} + E_{\eta^0}\right] , \tag{4.5}$$

JHEP06(2020)170

where the particle energies are given by eqs. (3.55)–(3.59). Using eq. (4.3), we can write eq. (4.5) as

$$\begin{aligned} V_1 = &-\frac{3}{4(4\pi)^2}\left[\frac{1}{\epsilon}+\frac{3}{2}+\log\left(\frac{\Lambda^2}{m_{\pi,0}^2}\right)\right][2B_0 m]^2 \\ &-\frac{1}{(4\pi)^2}\left[\frac{1}{\epsilon}+\frac{3}{2}+\log\left(\frac{\Lambda^2}{m_{K,0}^2}\right)\right][B_0(m+m_s)]^2 \\ &-\frac{1}{4(4\pi)^2}\left[\frac{1}{\epsilon}+\frac{3}{2}+\log\left(\frac{\Lambda^2}{m_{\eta,0}^2}\right)\right]\left[\frac{2B_0(m+2m_s)}{3}\right]^2 . \end{aligned} \tag{4.6}$$

The $\mathcal{O}(p^4)$ contribution from minus the static Lagrangian $\mathcal{L}_4^{\text{static}}$ is given by

$$V_1^{\text{static}} = -16L_6B_0^2(2m+m_s)^2 - 8L_8B_0^2(2m^2+m_s^2) - 4H_2B_0^2(2m^2+m_s^2) \tag{4.7}$$

After renormalization, the effective potential is

$$\begin{aligned} V_{\text{eff}} = &-f^2B_0(2m+m_s) - 16L_6^rB_0^2(2m+m_s)^2 - 8L_8^rB_0^2(2m^2+m_s^2) - 4H_2^rB_0^2(2m^2+m_s^2) \\ &-\left[\frac{1}{(4\pi)^2}\left(\frac{37}{18}+3\log\frac{\Lambda^2}{m_{\pi,0}^2}+\log\frac{\Lambda^2}{m_{K,0}^2}+\frac{1}{9}\log\frac{\Lambda^2}{m_{\eta,0}^2}\right)\right]B_0^2m^2 \\ &-\left[\frac{1}{(4\pi)^2}\left(\frac{11}{9}+2\log\frac{\Lambda^2}{m_{K,0}^2}+\frac{4}{9}\log\frac{\Lambda^2}{m_{\eta,0}^2}\right)\right]B_0^2mm_s \\ &-\left[\frac{1}{(4\pi)^2}\left(\frac{13}{18}+\log\frac{\Lambda^2}{m_{K,0}^2}+\frac{4}{9}\log\frac{\Lambda^2}{m_{\eta,0}^2}\right)\right]B_0^2m_s^2 . \end{aligned} \tag{4.8}$$

Using the renormalization group equations (2.17) for the couplings, we find that the effective potential is independent of the renormalization scale Λ. We note that the renormalized effective potential of eq. (4.8) is independent of the chemical potentials μ_I and μ_S. This independence is a result that we expect will generalize at next-to-next-to-leading order (NNLO) and higher orders. This is due to a general argument, namely the Silver Blaze property, that shows the isospin independence of the eigenvalues of the Dirac operator at finite isospin density (in the normal phase) [55] and consequently the isospin independence of the partition function and resulting thermodynamic quantities. While the original proof in ref. [55] did not include the strange chemical potential, we expect that it generalizes to systems with both isospin and strange chemical potentials.

4.2 Pion-condensed phase

The tree-level contribution to the effective potential is minus the static Lagrangian given in eq. (3.60)

$$V_0 = -f^2B_0(2m\cos\alpha + m_s) - \frac{1}{2}f^2\mu_I^2\sin^2\alpha . \tag{4.9}$$

The one-loop effective potential is

$$V_1 = \frac{1}{2}\int_p \left[E_{\pi^+}+E_{\pi^-}+E_{\pi^0}+E_{K^+}+E_{K^-}+E_{K^0}+E_{\bar{K}^0}+E_{\eta^0}\right] . \tag{4.10}$$

JHEP06(2020)170

where the energies are given by eqs. (3.77)–(3.81). The integrals of E_{π^0} and E_{η^0} can be calculated analytically in dimensional regularization using eq. (4.3). The remaining contributions require a little more work. Let us consider the contribution from the charged pions. In order to eliminate the divergences, their dispersion relations are expanded in powers of $1/p$ as

$$E_{\pi^+} + E_{\pi^-} = 2p + \frac{2(m_1^2 + m_2^2) + m_{12}^2}{4p} - \frac{8(m_1^4 + m_2^4) + 4(m_1^2 + m_2^2)m_{12}^2 + m_{12}^4}{64p^3} + \dots \quad (4.11)$$

To this order, the large-p behavior in eq. (4.11) is the same as the sum $E_1 + E_2$, where $E_1 = \sqrt{p^2 + m_1^2 + \frac{1}{4}m_{12}^2}$ and $E_2 = \sqrt{p^2 + m_2^2 + \frac{1}{4}m_{12}^2}$. For later convenience we introduce the masses $\tilde{m}_1^2 = m_1^2 + \frac{1}{4}m_{12}^2 = 2B_0 m\cos\alpha$, $\tilde{m}_2^2 = m_2^2 + \frac{1}{4}m_{12}^2 = 2B_0 m\cos\alpha + \mu_I^2\sin^2\alpha = m_3^2$, The integral over $E_{\pi^+} + E_{\pi^-} - E_1 - E_2$ is convergent in the ultraviolet and the subtraction integrals of E_1 and E_2 can be done analytically in dimensional regularization. We can then write

$$V_{1,\pi^+} + V_{1,\pi^-} = V_{1,\pi^+}^{\rm div} + V_{1,\pi^-}^{\rm div} + V_{1,\pi^+}^{\rm fin} + V_{1,\pi^-}^{\rm fin} \quad (4.12)$$

where

$$V_{1,\pi^+}^{\rm div} + V_{1,\pi^-}^{\rm div} = \frac{1}{2}\int_p [E_1 + E_2]\ , \quad (4.13)$$

$$V_{1,\pi^+}^{\rm fin} + V_{1,\pi^-}^{\rm fin} = \frac{1}{2}\int_p [E_{\pi^+} + E_{\pi^-} - E_1 - E_2]\ . \quad (4.14)$$

The contributions from the kaons can be calculated analytically as follows. Consider first the contribution from the charged kaon which is given by

$$V_{1,K^+} + V_{1,K^-} = \frac{1}{2}\int_P \log\left[(P^2 + m_4^2)(P^2 + m_5^2) + p_0^2 m_{45}^2\right]\ , \quad (4.15)$$

which can be rewritten as

$$V_{1,K^+} + V_{1,K^-} = \frac{1}{2}\int_P \log\left\{\left[P^2 + \frac{1}{2}(m_4^2 + m_5^2)\right]^2 + p_0^2 m_{45}^2 - \frac{1}{4}(m_4^2 - m_5^2)^2\right\}\ . \quad (4.16)$$

Since $m_4 = m_5$, the last term vanishes and the integrand can be factorized as

$$V_{1,K^+} + V_{1,K^-} = \frac{1}{2}\int_P \log\left[\left(p_0 + \frac{im_{45}}{2}\right)^2 + p^2 + m_4^2 + \frac{1}{4}m_{45}^2\right] \times \left[\left(p_0 - \frac{im_{45}}{2}\right)^2 + p^2 + m_4^2 + \frac{1}{4}m_{45}^2\right]\ . \quad (4.17)$$

Shifting integration variables in the two terms, $p_0 \to p_0 \mp \frac{im_{45}}{2}$, the integral simplifies to

$$V_{1,K^+} + V_{1,K^-} = \int_P \log\left[P^2 + m_4^2 + \frac{1}{4}m_{45}^2\right]\ . \quad (4.18)$$

JHEP06(2020)170

The contribution from the neutral kaons is obtained simply by replacing m_4 by m_6 and m_{45} by m_{67}. Since $\tilde{m}_2^2 = m_3^2$ and by defining $\tilde{m}_4^2 = m_4^2 + \frac{1}{4}m_{45}^2 = m_6^2 + \frac{1}{4}m_{67}^2 = B_0(m\cos\alpha + m_s) + \frac{1}{4}\mu_I^2\sin^2\alpha$, we can write the divergent part of the one-loop contribution as

$$\begin{aligned} V_1^{\text{div}} = &-\frac{1}{4(4\pi)^2}\left[\frac{1}{\epsilon}+\frac{3}{2}+\log\left(\frac{\Lambda^2}{\tilde{m}_1^2}\right)\right][2B_0 m\cos\alpha]^2 \\ &-\frac{1}{2(4\pi)^2}\left[\frac{1}{\epsilon}+\frac{3}{2}+\log\left(\frac{\Lambda^2}{m_3^2}\right)\right]\left[2B_0 m\cos\alpha+\mu_I^2\sin^2\alpha\right]^2 \\ &-\frac{1}{(4\pi)^2}\left[\frac{1}{\epsilon}+\frac{3}{2}+\log\left(\frac{\Lambda^2}{\tilde{m}_4^2}\right)\right]\left[B_0(m\cos\alpha+m_s)+\frac{1}{4}\mu_I^2\sin^2\alpha\right]^2 \\ &-\frac{1}{4(4\pi)^2}\left[\frac{1}{\epsilon}+\frac{3}{2}+\log\left(\frac{\Lambda^2}{m_8^2}\right)\right]\left[\frac{2B_0(m\cos\alpha+2m_s)}{3}\right]^2, \end{aligned} \tag{4.19}$$

The static part of the Lagrangian $\mathcal{L}_4$ as a function of α is

$$\begin{aligned} V_1^{\text{static}} = &-(4L_1+4L_2+2L_3)\mu_I^4\sin^4\alpha - 8L_4B_0(2m\cos\alpha+m_s)\mu_I^2\sin^2\alpha \\ &-8L_5B_0m\mu_I^2\cos\alpha\sin^2\alpha - 16L_6B_0^2(2m\cos\alpha+m_s)^2 \\ &-8L_8B_0^2(2m^2\cos 2\alpha+m_s^2) - 4H_2B_0^2(2m^2+m_s^2). \end{aligned} \tag{4.20}$$

The renormalized one-loop effective potential $V_{\text{eff}} = V_0 + V_1 + V_1^{\text{static}}$ is given by the sum of eqs. (4.9), (4.19), and (4.20) then reads

$$\begin{aligned} V_{\text{eff}} = &-f^2B_0(2m\cos\alpha+m_s) - \frac{1}{2}f^2\mu_I^2\sin^2\alpha - (4L_1^r+4L_2^r+2L_3^r)\mu_I^4\sin^4\alpha \\ &-8L_4^rB_0(2m\cos\alpha+m_s)\mu_I^2\sin^2\alpha - 8L_5^rB_0m\mu_I^2\cos\alpha\sin^2\alpha \\ &-16L_6^rB_0^2(2m\cos\alpha+m_s)^2 - 8L_8^rB_0^2(2m^2\cos 2\alpha+m_s^2) - 4H_2^rB_0^2(2m^2+m_s^2) \\ &-\frac{1}{4(4\pi)^2}\left[\frac{1}{2}+\log\left(\frac{\Lambda^2}{\tilde{m}_1^2}\right)\right][2B_0m\cos\alpha]^2 \\ &-\frac{1}{2(4\pi)^2}\left[\frac{1}{2}+\log\left(\frac{\Lambda^2}{m_3^2}\right)\right]\left[2B_0m\cos\alpha+\mu_I^2\sin^2\alpha\right]^2 \\ &-\frac{1}{(4\pi)^2}\left[\frac{1}{2}+\log\left(\frac{\Lambda^2}{\tilde{m}_4^2}\right)\right]\left[B_0(m\cos\alpha+m_s)+\frac{1}{4}\mu_I^2\sin^2\alpha\right]^2 \\ &-\frac{1}{4(4\pi)^2}\left[\frac{1}{2}+\log\left(\frac{\Lambda^2}{m_8^2}\right)\right]\left[\frac{2B_0(m\cos\alpha+2m_s)}{3}\right]^2 + V_{1,\pi^+}^{\text{fin}} + V_{1,\pi^-}^{\text{fin}}. \end{aligned} \tag{4.21}$$

Again, it can be verified that the NLO effective potential is independent of the scale Λ. it is also explicitly independent of the strangeness chemical potential μ_S.

4.3 Charged kaon-condensed phase

The tree-level contribution to the effective potential is

$$V_0 = -f^2B_0\left[m+(m+m_s)\cos\alpha\right] - \frac{1}{2}f^2\left(\frac{1}{2}\mu_I+\mu_S\right)^2\sin^2\alpha. \tag{4.22}$$

JHEP06(2020)170

The one-loop effective potential is

$$V_1 = \frac{1}{2}\int_p \left[E_{\pi^+} + E_{\pi^-} + E_{\pi^0} + E_{K^+} + E_{K^-} + E_{K^0} + E_{\bar{K}^0} + E_{\eta^0}\right] . \tag{4.23}$$

The contributions from $\pi^\pm$, $K^\pm$, K^0 and $\bar{K}^0$ can be treated as in the previous section and it is only the terms $V_{1,K^\pm}$ that require a subtraction term. The relevant masses are defined as

$$\tilde{m}_1^2 = m_1^2 + \frac{1}{4}m_{12}^2 = \frac{1}{2}B_0[3m - m_s + (m+m_s)\cos\alpha] + \frac{1}{4}\left(\frac{1}{2}\mu_I + \mu_S\right)^2 \sin^2\alpha\,, \tag{4.24}$$

$$\tilde{m}_4^2 = m_4^2 + \frac{1}{4}m_{45}^2 = B_0(m+m_s)\cos\alpha\,, \tag{4.25}$$

$$\tilde{m}_5^2 = m_5^2 + \frac{1}{4}m_{45}^2 = B_0(m+m_s)\cos\alpha + \left(\frac{1}{2}\mu_I + \mu_S\right)^2 \sin^2\alpha\,, \tag{4.26}$$

$$\tilde{m}_6^2 = m_6^2 + \frac{1}{4}m_{67}^2 = \frac{1}{2}B_0(m+m_s)(1+\cos\alpha) + \frac{1}{4}\left(\frac{1}{2}\mu_I + \mu_S\right)^2 \sin^2\alpha\,. \tag{4.27}$$

The contribution from the mixed π^0 and η^0 is given by

$$\begin{aligned} V_{1,\pi^0} + V_{1,\eta^0} &= \frac{1}{2}\int_P \log\left[(P^2+m_3^2)(P^2+m_8^2) - m_{38}^4\right] \\ &= \frac{1}{2}\int_P \log\left[P^2+\tilde{m}_3^2\right] + \log[P^2+\tilde{m}_8^2]\,, \end{aligned} \tag{4.28}$$

where the new masses are defined as

$$\tilde{m}_{3,8}^2 = \frac{1}{2}\left[m_3^2 + m_8^2 \pm \sqrt{(m_3^2-m_8^2)^2 + 4m_{38}^4}\right] . \tag{4.29}$$

This yields

$$\begin{aligned} V_1 = &-\frac{1}{2(4\pi)^2}\left[\frac{1}{\epsilon}+\frac{3}{2}+\log\left(\frac{\Lambda^2}{\tilde{m}_1^2}\right)\right]\left\{\frac{1}{2}B_0[(3m-m_s+(m+m_s)\cos\alpha] \right. \\ &\qquad \left. +\frac{1}{4}\left(\frac{1}{2}\mu_I+\mu_S\right)^2\sin^2\alpha\right\}^2 \\ &-\frac{1}{4(4\pi)^2}\left[\frac{1}{\epsilon}+\frac{3}{2}+\log\left(\frac{\Lambda^2}{\tilde{m}_4^2}\right)\right]\left[B_0^2(m+m_s)^2\cos^2\alpha\right] \\ &-\frac{1}{4(4\pi)^2}\left[\frac{1}{\epsilon}+\frac{3}{2}+\log\left(\frac{\Lambda^2}{\tilde{m}_5^2}\right)\right]\left[B_0(m+m_s)\cos\alpha+\left(\frac{1}{2}\mu_I+\mu_S\right)^2\sin^2\alpha\right]^2 \\ &-\frac{1}{2(4\pi)^2}\left[\frac{1}{\epsilon}+\frac{3}{2}+\log\left(\frac{\Lambda^2}{\tilde{m}_6^2}\right)\right]\left[\frac{1}{2}B_0(m+m_s)(1+\cos\alpha)+\frac{1}{4}\left(\frac{1}{2}\mu_I+\mu_S\right)^2\sin^2\alpha\right]^2 \\ &-\frac{1}{4(4\pi)^2}\left[\frac{1}{\epsilon}+\frac{3}{2}+\log\left(\frac{\Lambda^2}{\tilde{m}_3^2}\right)\right]\tilde{m}_3^4 - \frac{1}{4(4\pi)^2}\left[\frac{1}{\epsilon}+\frac{3}{2}+\log\left(\frac{\Lambda^2}{\tilde{m}_8^2}\right)\right]\tilde{m}_8^4 . \end{aligned} \tag{4.30}$$

JHEP06(2020)170

The static part of the Lagrangian $\mathcal{L}_4$ as a function of α is

$$\begin{aligned} V_1^{\text{static}} = & -(4L_1+4L_2+2L_3)\left(\frac{1}{2}\mu_I+\mu_S\right)^4\sin^4\alpha \\ & -8L_4B_0[m+(m+m_s)\cos\alpha]\left(\frac{1}{2}\mu_I+\mu_S\right)^2\sin^2\alpha \\ & -4L_5B_0(m+m_s)\left(\frac{1}{2}\mu_I+\mu_S\right)^2\cos\alpha\sin^2\alpha-16L_6B_0^2[m+(m+m_s)\cos\alpha]^2 \\ & -4L_8B_0^2(3m^2-2mm_s+m_s^2+(m+m_s)^2\cos 2\alpha)-4H_2B_0^2(2m^2+m_s^2)\,. \end{aligned} \tag{4.31}$$

After renormalization, the effective potential is

$$\begin{aligned} V_{\text{eff}} = & -f^2B_0\left[m+(m+m_s)\cos\alpha\right]-\frac{1}{2}f^2\left(\frac{1}{2}\mu_I+\mu_S\right)^2\sin^2\alpha \\ & -(4L_1^r+4L_2^r+2L_3^r)\left(\frac{1}{2}\mu_I+\mu_S\right)^4\sin^4\alpha \\ & -8L_4^rB_0[m+(m+m_s)\cos\alpha]\left(\frac{1}{2}\mu_I+\mu_S\right)^2\sin^2\alpha \\ & -4L_5^rB_0(m+m_s)\left(\frac{1}{2}\mu_I+\mu_S\right)^2\cos\alpha\sin^2\alpha-16L_6^rB_0[m+(m+m_s)\cos\alpha]^2 \\ & -4L_8^rB_0^2(3m^2-2mm_s+m_s^2+(m+m_s)^2\cos 2\alpha)-4H_2^rB_0^2(2m^2+m_s^2) \\ & -\frac{1}{2(4\pi)^2}\left[\frac{1}{2}+\log\left(\frac{\Lambda^2}{\tilde{m}_1^2}\right)\right]\left\{\frac{1}{2}B_0[(3m-m_s+(m+m_s)\cos\alpha]\right. \\ & \qquad\left.+\frac{1}{4}\left(\frac{1}{2}\mu_I+\mu_S\right)^2\sin^2\alpha\right\}^2 \\ & -\frac{1}{4(4\pi)^2}\left[\frac{1}{2}+\log\left(\frac{\Lambda^2}{\tilde{m}_4^2}\right)\right]\left[B_0^2(m+m_s)^2\cos^2\alpha\right] \\ & -\frac{1}{4(4\pi)^2}\left[\frac{1}{2}+\log\left(\frac{\Lambda^2}{\tilde{m}_5^2}\right)\right]\left[B_0(m+m_s)\cos\alpha+\left(\frac{1}{2}\mu_I+\mu_S\right)^2\sin^2\alpha\right]^2 \\ & -\frac{1}{2(4\pi)^2}\left[\frac{1}{2}+\log\left(\frac{\Lambda^2}{\tilde{m}_6^2}\right)\right]\left[\frac{1}{2}B_0(m+m_s)(1+\cos\alpha)+\frac{1}{4}\left(\frac{1}{2}\mu_I+\mu_S\right)^2\sin^2\alpha\right]^2 \\ & -\frac{1}{4(4\pi)^2}\left[\frac{1}{2}+\log\left(\frac{\Lambda^2}{\tilde{m}_3^2}\right)\right]\tilde{m}_3^4-\frac{1}{4(4\pi)^2}\left[\frac{1}{2}+\log\left(\frac{\Lambda^2}{\tilde{m}_8^2}\right)\right]\tilde{m}_8^4+V_{1,K^+}^{\text{fin}}+V_{1,K^-}^{\text{fin}}\,, \end{aligned} \tag{4.32}$$

where the subtraction terms and energies are defined by

$$V_{1,K^+}^{\text{fin}}+V_{1,K^-}^{\text{fin}} = \frac{1}{2}\int_p\left[E_{K^+}+E_{K^-}-E_4-E_5\right]\,, \tag{4.33}$$

$$E_{4,5} = \sqrt{p^2+\tilde{m}_{4,5}^2}\,, \tag{4.34}$$

with $\tilde{m}_{4,5}$ given by eqs. (4.25)–(4.26).

The effective potential depends only on the combination $\frac{1}{2}\mu_I+\mu_S$ as is evident by inspection. Using the expressions for the running couplings, eq. (2.17), the scale dependence in the final results for the effective potential, eqs. (4.8), (4.21), and (4.32) cancels.

JHEP06(2020)170

5 Thermodynamic functions

In this section, we derive the thermodynamic functions from the effective potential. We will focus on the pion-condensed phase since we are interested in comparing our results with lattice simulations.

5.1 Pion-condensed phase

The pressure P is given by $-V_{\rm eff}$. In the pion-condensed phase, we get from eq. (4.21)

$$\begin{aligned}
P =\ & f^2 B_0(2m\cos\alpha + m_s) + \frac{1}{2}f^2\mu_I^2\sin^2\alpha \\
& + \left[4L_1^r + 4L_2^r + 2L_3^r + \frac{1}{16(4\pi)^2}\left(\frac{9}{2} + 8\log\frac{\Lambda^2}{m_3^2} + \log\frac{\Lambda^2}{\tilde{m}_4^2}\right)\right]\mu_I^4\sin^4\alpha \\
& + \left[8L_4^r + \frac{1}{2(4\pi)^2}\left(\frac{1}{2} + \log\frac{\Lambda^2}{\tilde{m}_4^2}\right)\right] B_0(2m\cos\alpha + m_s)\mu_I^2\sin^2\alpha \\
& + \left[8L_5^r + \frac{1}{2(4\pi)^2}\left(\frac{3}{2} + 4\log\frac{\Lambda^2}{m_3^2} - \log\frac{\Lambda^2}{\tilde{m}_4^2}\right)\right] B_0 m\mu_I^2\cos\alpha\sin^2\alpha \\
& + \left[16L_6^r + 8L_8^r + 4H_2^r + \frac{1}{(4\pi)^2}\left(\frac{13}{18} + \log\frac{\Lambda^2}{\tilde{m}_4^2} + \frac{4}{9}\log\frac{\Lambda^2}{m_8^2}\right)\right] B_0^2 m_s^2 \\
& + \left[64L_6^r + \frac{1}{(4\pi)^2}\left(\frac{11}{9} + 2\log\frac{\Lambda^2}{\tilde{m}_4^2} + \frac{4}{9}\log\frac{\Lambda^2}{m_8^2}\right)\right] B_0^2 m m_s\cos\alpha \\
& + \left[64L_6^r + 16L_8^r + 8H_2^r + \frac{1}{(4\pi)^2}\left(\frac{37}{18} + \log\frac{\Lambda^2}{\tilde{m}_1^2} + \right.\right. \\
& \qquad \left.\left. + 2\log\frac{\Lambda^2}{m_3^2} + \log\frac{\Lambda^2}{\tilde{m}_4^2} + \frac{1}{9}\log\frac{\Lambda^2}{m_8^2}\right)\right] B_0^2 m^2\cos^2\alpha - \left[16L_8^r - 8H_2^r\right] B_0^2 m^2\sin^2\alpha \\
& - V_{1,\pi^+}^{\rm fin} - V_{1,\pi^-}^{\rm fin}\,,
\end{aligned} \tag{5.1}$$

The isospin density is given by

$$\begin{aligned}
n_I =\ & -\frac{\partial V_{\rm eff}}{\partial\mu_I} \\
=\ & f^2\mu_I\sin^2\alpha + \left[16L_1^r + 16L_2^r + 8L_3^r + \frac{1}{4(4\pi)^2}\left(8\log\frac{\Lambda^2}{m_3^2} + \log\frac{\Lambda^2}{\tilde{m}_4^2}\right)\right]\mu_I^3\sin^4\alpha \\
& + \left[16L_4^r + \frac{1}{(4\pi)^2}\log\frac{\Lambda^2}{\tilde{m}_4^2}\right] B_0(2m\cos\alpha + m_s)\mu_I\sin^2\alpha \\
& + \left[16L_5^r + \frac{1}{(4\pi)^2}\left(4\log\frac{\Lambda^2}{m_3^2} - \log\frac{\Lambda^2}{\tilde{m}_4^2}\right)\right] B_0 m\mu_I\cos\alpha\sin^2\alpha - \frac{\partial V_{1,\pi^+}^{\rm fin}}{\partial\mu_I} - \frac{\partial V_{1,\pi^-}^{\rm fin}}{\partial\mu_I}\,.
\end{aligned} \tag{5.2}$$

The energy density is given by

$$\epsilon = -P + \mu_i n_i\,. \tag{5.3}$$

where $n_i = -\frac{\partial V_{\rm eff}}{\partial\mu_i}$ is the charge density associated with the chemical potential μ_i. In the pion-condensed phase it takes the following form

$$\epsilon = -P + \mu_I n_I\,. \tag{5.4}$$

JHEP06(2020)170

since the effective potential is independent of $\mu_S = 0$ in this phase. Using eqs. (4.21) and (5.2), we find the following energy density

$$
\begin{aligned}
\epsilon = & -f^2 B_0(2m\cos\alpha + m_s) + \frac{1}{2} f^2 \mu_I \sin^2\alpha \\
& + \left[12L_1^r + 12L_2^r + 6L_3^r + \frac{1}{(4\pi)^2}\left(-\frac{9}{32} + \frac{3}{2}\log\frac{\Lambda^2}{m_3^2} + \frac{3}{16}\log\frac{\Lambda^2}{\tilde{m}_4^2}\right)\right]\mu_I^4 \sin^4\alpha \\
& + \left[8L_4^r + \frac{1}{2(4\pi)^2}\left(-\frac{1}{2} + \log\frac{\Lambda^2}{\tilde{m}_4^2}\right)\right] B_0(2m\cos\alpha + m_s)\mu_I^2 \sin^2\alpha \\
& + \left[8L_5^r + \frac{1}{2(4\pi)^2}\left(-\frac{3}{2} + 4\log\frac{\Lambda^2}{m_3^2} - \log\frac{\Lambda^2}{\tilde{m}_4^2}\right)\right] B_0 m \mu_I^2 \cos\alpha \sin^2\alpha \\
& - \left[16L_6^r + 8L_8^r + 4H_2^r + \frac{1}{(4\pi)^2}\left(\frac{13}{18} + \log\frac{\Lambda^2}{\tilde{m}_4^2} + \frac{4}{9}\log\frac{\Lambda^2}{m_8^2}\right)\right] B_0^2 m_s^2 \\
& - \left[64L_6^r + \frac{1}{(4\pi)^2}\left(\frac{11}{9} + 2\log\frac{\Lambda^2}{\tilde{m}_4^2} + \frac{4}{9}\log\frac{\Lambda^2}{m_8^2}\right)\right] B_0^2 m m_s \cos\alpha \\
& - \left[64L_6^r + 16L_8^r + 8H_2^r + \frac{1}{(4\pi)^2}\left(\frac{37}{18} + \log\frac{\Lambda^2}{\tilde{m}_1^2} + 2\log\frac{\Lambda^2}{m_3^2} + \log\frac{\Lambda^2}{\tilde{m}_4^2} + \frac{1}{9}\log\frac{\Lambda^2}{m_8^2}\right)\right] \\
& \times B_0^2 m^2 \cos^2\alpha + [16L_8^r - 8H_2^r] B_0^2 m^2 \sin^2\alpha + V_{1,\pi^+}^{\text{fin}} + V_{1,\pi^-}^{\text{fin}} - \mu_I \frac{\partial V_{1,\pi^+}^{\text{fin}}}{\partial \mu_I} - \mu_I \frac{\partial V_{1,\pi^-}^{\text{fin}}}{\partial \mu_I},
\end{aligned}
\tag{5.5}
$$

5.2 Large-m_s limit

We are interested in the large-m_s limit of our three-flavor results for thermodynamic quantities. In this limit, general effective field theory arguments tell us that the mesonic degrees of freedom containing the s-quark decouple. Thus one should recover the two-flavor results of ref. [48] with modified couplings. The modified couplings then contain the loop effects from integrating out kaons and the eta.

The one-loop expressions for the pion-decay constant and the light-quark condensate in the vacuum are given by [10]

$$
\begin{aligned}
f_\pi^2 = & f^2\left[1 + \left(8L_4^r + 8L_5^r + \frac{2}{(4\pi)^2}\log\frac{\Lambda^2}{m_{\pi,0}^2}\right)\frac{m_{\pi,0}^2}{f^2}\right. \\
& \left. + \left(16L_4^r + \frac{1}{(4\pi)^2}\log\frac{\Lambda^2}{m_{K,0}^2}\right)\frac{m_{K,0}^2}{f^2}\right]
\end{aligned}
\tag{5.6}
$$

$$
\begin{aligned}
\langle\bar{\psi}\psi\rangle = & -f^2 B_0\left[1 + \left(16L_6^r + 4L_8^r + 4H_2^r + \frac{3}{2(4\pi)^2}\log\frac{\Lambda^2}{m_{\pi,0}^2}\right)\frac{m_{\pi,0}^2}{f^2}\right. \\
& \left. + \left(32L_6^r + \frac{1}{(4\pi)^2}\log\frac{\Lambda^2}{m_{K,0}^2}\right)\frac{m_{K,0}^2}{f^2} + \frac{m_{\eta,0}^2}{6(4\pi)^2 f^2}\log\frac{\Lambda^2}{m_{\eta,0}^2}\right].
\end{aligned}
\tag{5.7}
$$

JHEP06(2020)170

The loop corrections involve pions, kaons, and etas. Integrating out the s-quark corresponds to setting $m = 0$ or ignoring the pionic loop corrections. This yields

$$\tilde{f}^2 = f^2 \left[1 + \left(16 L_4^r + \frac{1}{(4\pi)^2} \log \frac{\Lambda^2}{\tilde{m}_{K,0}^2} \right) \frac{\tilde{m}_{K,0}^2}{f^2} \right] , \tag{5.8}$$

$$\langle \bar{\psi}\psi \rangle = -f^2 B_0 \left[1 + \left(32 L_6^r + \frac{1}{(4\pi)^2} \log \frac{\Lambda^2}{\tilde{m}_{K,0}^2} \right) \frac{\tilde{m}_{K,0}^2}{f^2} + \frac{\tilde{m}_{\eta,0}^2}{6(4\pi)^2 f^2} \log \frac{\Lambda^2}{\tilde{m}_{\eta,0}^2} \right] , \tag{5.9}$$

where the masses are $\tilde{m}_{K,0}^2 = B_0 m_s$ and $\tilde{m}_{\eta,0}^2 = \frac{4B_0 m_s}{3}$. Defining $\tilde{B}_0$ via $\langle \bar{\psi}\psi \rangle = -\tilde{f}^2 \tilde{B}_0$ yields

$$\tilde{B}_0 = B_0 \left[1 - (16 L_4^r - 32 L_6^r) \frac{\tilde{m}_{K,0}^2}{f^2} + \frac{\tilde{m}_{\eta,0}^2}{6(4\pi)^2 f^2} \log \frac{\Lambda^2}{\tilde{m}_{\eta,0}^2} \right] . \tag{5.10}$$

Using the renormalization group equations for L_4^r and L_6^r, one verifies that eqs. (5.8) and (5.10) are independent of the scale Λ. Moreover, in ref. [10], the authors derived the relations among the renormalized couplings in two - and three-flavor χPT. The relevant relations are

$$l_1^r = 4 L_1^r + 2 L_3^r + \frac{1}{48(4\pi)^2} \left[\log \frac{\Lambda^2}{\tilde{m}_{K,0}^2} - 1 \right] , \tag{5.11}$$

$$l_2^r = 4 L_2^r + \frac{1}{24} \frac{1}{(4\pi)^2} \left[\log \frac{\Lambda^2}{\tilde{m}_{K,0}^2} - 1 \right] , \tag{5.12}$$

$$l_3^r = -8 L_4^r - 4 L_5^r + 16 L_6^r + 8 L_8^r + \frac{1}{36(4\pi)^2} \left[\log \frac{\Lambda^2}{\tilde{m}_{\eta,0}^2} - 1 \right] \tag{5.13}$$

$$l_4^r = 8 L_4^r + 4 L_5^r + \frac{1}{4(4\pi)^2} \left[\log \frac{\Lambda^2}{\tilde{m}_{K,0}^2} - 1 \right] , \tag{5.14}$$

$$h_1^r = 8 L_4^r + 4 L_5^r - 4 L_8^r + 2 H_2^r + \frac{1}{4(4\pi)^2} \left[\log \frac{\Lambda^2}{\tilde{m}_{K,0}^2} - 1 \right] . \tag{5.15}$$

The relations between the renormalized couplings l_i^r, h_i^r and the low-energy constants $\bar{l}_i, \bar{h}_i$ in two-flavor χPT are

$$l_i^r(\Lambda) = \frac{\gamma_i}{2(4\pi)^2} \left[\bar{l}_i + \log \frac{2B_0 m}{\Lambda^2} \right] , \qquad h_i^r(\Lambda) = \frac{\delta_i}{2(4\pi)^2} \left[\bar{h}_i + \log \frac{2B_0 m}{\Lambda^2} \right] , \tag{5.16}$$

where $\gamma_1 = \frac{1}{3}$, $\gamma_2 = \frac{2}{3}$, $\gamma_3 = -\frac{1}{2}$, $\gamma_4 = 2$, and $\delta_1 = 2$ [9]. Using the renormalization group equations for renormalized couplings, one finds that the Λ-dependence are the same on the left - and right-hand sides of eqs. (5.11)–(5.15).

The low-energy limit of eqs. (5.1), (5.2), and (5.5) are then obtained as follows. We expand them in powers of $1/m_s$, express the result using eqs. (5.8), and (5.10)–(5.16). The

JHEP06(2020)170

pressure is

$$
\begin{aligned}
P = {} & 2\tilde{f}^2\tilde{B}_0 m\cos\alpha + \frac{1}{2}\tilde{f}^2\mu_I^2\sin^2\alpha - \frac{4}{(4\pi)^2}\left[-\bar{h}_1+\bar{l}_4\right]B_0^2m^2 \\
& + \frac{1}{(4\pi)^2}\left[\frac{3}{2}-\bar{l}_3+4\bar{l}_4+\log\left(\frac{2B_0m}{\tilde{m}_1^2}\right)+2\log\frac{2B_0m}{m_3^2}\right]B_0^2m^2\cos^2\alpha \\
& + \frac{1}{(4\pi)^2}\left[\frac{1}{2}+\bar{l}_4+\log\frac{2B_0m}{m_3^2}\right]2B_0m\mu_I^2\cos\alpha\sin^2\alpha \\
& + \frac{1}{2(4\pi)^2}\left[\frac{1}{2}+\frac{1}{3}\bar{l}_1+\frac{2}{3}\bar{l}_2+\log\frac{2B_0m}{m_3^2}\right]\mu_I^4\sin^4\alpha - V_{1,\pi^+}^{\text{fin}} - V_{1,\pi^-}^{\text{fin}}\,,
\end{aligned}
\tag{5.17}
$$

the isospin density is

$$
\begin{aligned}
n_I = {} & \tilde{f}^2\mu_I\sin^2\alpha + \frac{2}{(4\pi)^2}\left[\bar{l}_4+\log\frac{2B_0m}{m_3^2}\right]2B_0m\mu_I\cos\alpha\sin^2\alpha \\
& + \frac{2}{(4\pi)^2}\left[\frac{1}{3}\bar{l}_1+\frac{2}{3}\bar{l}_2+\log\frac{2B_0m}{m_3^2}\right]\mu_I^3\sin^4\alpha - \frac{\partial V_{1,\pi^+}^{\text{fin}}}{\partial\mu_I} - \frac{\partial V_{1,\pi^-}^{\text{fin}}}{\partial\mu_I}\,,
\end{aligned}
\tag{5.18}
$$

and the energy density is

$$
\begin{aligned}
\epsilon = {} & -2\tilde{f}^2\tilde{B}_0 m\cos\alpha + \frac{1}{2}\tilde{f}^2\mu_I^2\sin^2\alpha + \frac{4}{(4\pi)^2}\left[-\bar{h}_1+\bar{l}_4\right]B_0^2m^2 \\
& - \frac{1}{(4\pi)^2}\left[\frac{3}{2}-\bar{l}_3+4\bar{l}_4+\log\left(\frac{2B_0m}{\tilde{m}_1^2}\right)+2\log\left(\frac{2B_0m}{m_3^2}\right)\right]B_0^2m^2\cos^2\alpha \\
& - \frac{1}{(4\pi)^2}\left[\frac{1}{2}-\bar{l}_4-\log\frac{2B_0m}{m_3^2}\right]2B_0m\mu_I^2\cos\alpha\sin^2\alpha \\
& - \frac{1}{2(4\pi)^2}\left[\frac{1}{2}-\bar{l}_1-2\bar{l}_2-3\log\frac{2B_0m}{m_3^2}\right]\mu_I^4\sin^4\alpha + V_{1,\pi^+}^{\text{fin}} + V_{1,\pi^-}^{\text{fin}} \\
& - \mu_I\frac{\partial V_{1,\pi^+}^{\text{fin}}}{\partial\mu_I} - \mu_I\frac{\partial V_{1,\pi^-}^{\text{fin}}}{\partial\mu_I}\,.
\end{aligned}
\tag{5.19}
$$

Up to different notation ($2B_0m \to m^2$), the results for P, n_I, and ϵ are of the same form as the two-flavor results derived in [48] with renormalized parameters $\tilde{B}_0$ and $\tilde{f}$. (In two-flavor χPT m is the tree level pion mass [48].)

6 Results and discussion

In this section, we study the (tree-level) quasiparticle masses, isospin density, pressure and the equation of state. In order to evaluate these quantities, we need the numerical values of the low-energy constants (L_i) as well as the meson masses and decay constants. The low-energy constants have been determined experimentally, with the following values and uncertainties at the scale $\mu = m_\rho$, where $\Lambda^2 = 4\pi e^{-\gamma_E}\mu^2$ [59], where m_ρ is the mass of the

JHEP06(2020)170

ρ meson,

$$L_1^r = (1.0 \pm 0.1) \times 10^{-3}\,, \qquad L_2^r = (1.6 \pm 0.2) \times 10^{-3}\,, \tag{6.1}$$
$$L_3^r = (-3.8 \pm 0.3) \times 10^{-3}\,, \qquad L_4^r = (0.0 \pm 0.3) \times 10^{-3}\,, \tag{6.2}$$
$$L_5^r = (1.2 \pm 0.1) \times 10^{-3} \qquad L_6^r = (0.0 \pm 0.4) \times 10^{-3}\,, \tag{6.3}$$
$$L_7^r = (-0.4 \pm 0.2) \times 10^{-3} \qquad L_8^r = (0.5 \pm 0.2) \times 10^{-3}\,. \tag{6.4}$$

Since we are mainly interested in comparing our results to the predictions of the lattice simulations in refs. [43], we will use their values for the pion and kaon masses as well as the pion and kaon decay constants. With uncertainties, they are given by [58]

$$m_\pi = 131 \pm 3\text{MeV}\,, \qquad m_K = 481 \pm 10\text{MeV}\,, \tag{6.5}$$
$$f_\pi = \frac{128 \pm 3}{\sqrt{2}}\text{MeV}\,, \qquad f_K = \frac{150 \pm 3}{\sqrt{2}}\text{MeV}\,. \tag{6.6}$$

These uncertainties (in the masses and decay constants) arise due to lattice discretization errors and consequently differ slightly from their experimental values. Since we have three parameters in the Lagrangian, $B_0 m$, $B_0 m_s$, and f, we need to pick three observables from the set above, and we choose m_π, m_K, and f_π.

The relevant meson masses and the pion decay constants at one-loop are given by eqs. (A.1), (A.2), and (A.3) in terms of the parameters $B_0 m$, $B_0 m_s$ and f at next-to-leading order. Using the lattice values given above, we can solve for $B_0 m$, $B_0 m_s$, and f. This yields

$$f^{\text{cen}} = 75.16\,\text{MeV}\,, \qquad f^{\text{low}} = 79.88\,\text{MeV}\,, \qquad f^{\text{high}} = 70.44\,\text{MeV}\,, \tag{6.7}$$
$$m^{\text{low}}_{\pi,\text{tree}} = 148.45\,\text{MeV}\,, \qquad m^{\text{cen}}_{\pi,\text{tree}} = 131.28\,\text{MeV}\,, \qquad m^{\text{high}}_{\pi,\text{tree}} = 115.93\,\text{MeV}\,, \tag{6.8}$$
$$m^{\text{cen}}_{K,\text{tree}} = 520.65\,\text{MeV}\,, \qquad m^{\text{low}}_{K,\text{tree}} = 617.35\,\text{MeV}\,, \qquad m^{\text{high}}_{K,\text{tree}} = 437.84\,\text{MeV}\,, \tag{6.9}$$

where the subscripts indicate that the values correspond to the central, minimum, and maximum values of the low-energy constants. Using the one-loop χPT expression for the f_K, eq. (A.4), we find $f_K = 113.9\,\text{MeV}$ for the central values, which is off by approximately 7% compared to the lattice value of $f_K = \frac{150}{\sqrt{2}} = 106.1\,\text{MeV}$. The uncertainties in the LECs, L_i^r, the pion mass, m_π, the pion decay constant, f_π, and the kaon mass, m_K, lead to uncertainties in $B_0 m$, $B_0 m_s$ and f. These uncertainties are dominated by the uncertainties in the LECs with the uncertainty in the lattice parameters contributing the least. Additionally, it turns out that the lowest values of LECs calculated after including the LEC uncertainty leads to unphysical values of the η mass. As such we were forced to choose the lowest values of the LECs using 0.46 times the uncertainties leading to the results in eq. (6.7).

The thermodynamic quantities are functions of the effective potential evaluated at its minimum as a function of α for given values of the isospin and strange chemical potentials. Hence, we must solve the equation

$$\frac{\partial V_{\text{eff}}}{\partial \alpha} = 0\,. \tag{6.10}$$

JHEP06(2020)170

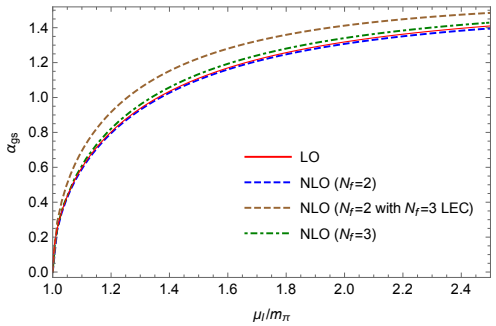

Figure 1. $\alpha_{\rm gs}$ as a function of μ_I/m_π at LO (red), at NLO with two flavors (blue), NLO with three flavors (green), and NLO with two flavors and three-flavor LECs (brown). See main text for details.

In figure 1, we show the solution to eq. (6.10) as function of the isospin chemical potential μ_I and $\mu_S = 0$. The red curve is the tree-level result, while the blue curve is the one-loop result in two-flavor χPT, the green curve is the one-loop result in three-flavor χPT and the brown curve is the one-loop result in two-flavor χPT using three-flavor LECs. In section 6.3, we use $\alpha_{\rm gs}$ to calculate the pressure, isospin density and the equation of state.

6.1 Phase diagram

We find that $\alpha_{\rm gs}$ becomes non-zero when $|\mu_I| > m_\pi$. In order to show that the transition from the vacuum phase to the Bose-condensed phases occurs at a critical chemical potential equal to the physical pion mass, we expand the effective potential in a power series in α around $\alpha = 0$ up to order α^4 to obtain an effective Landau-Ginzburg energy functional [53],

$$V_{\rm eff}^{\rm LG} = a_0 + a_2\alpha^2 + a_4\alpha^4 + \mathcal{O}(\alpha^6)\,. \tag{6.11}$$

As pointed out before, in the charged pion-condensed phase, $V_{\rm eff}$ and therefore the coefficients are independent of μ_S. Similarly, in the charged kaon-condensed phase, they only depend on the combination $\frac{1}{2}\mu_I + \mu_S$, and in the neutral kaon-condensed phase, only on the combination $-\frac{1}{2}\mu_I + \mu_S$, Using the expressions for the pion mass m_π (A.1) and the pion-decay constant f_π, (A.3), it can be shown that in the pion-condensed phase (see ref. [48] for details)

$$a_2(\mu_I) = \frac{1}{2}f_\pi^2\left[m_\pi^2 - \mu_I^2\right]\,. \tag{6.12}$$

The critical isospin chemical potential μ_I^c is defined by the vanishing of $a_2(\mu_I)$, and eq. (6.12) shows that $|\mu_I^c| = m_\pi$. Moreover, using the techniques in ref. [53] it can be shown that $a_4(\mu_I^c) > 0$, implying that the transition from the vacuum phase to a pion-condensed phase is second order located at $\mu_I^c = \pm m_\pi$.[7] Similarly, in the charged kaon-condensed phase, we find

$$a_2\left(\mu_I/2 + \mu_S\right) = \frac{1}{2}f_K^2\left[m_K^2 - \left(\frac{1}{2}\mu_I + \mu_S\right)^2\right]\,, \tag{6.13}$$

[7] If $a_4(\mu_I^c) < 0$, the transition is first order.

JHEP06(2020)170

where m_K is the physical kaon mass, whose one-loop expression is given by eq. (A.2). The critical chemical potential is again given by the vanishing of a_2, i.e. $|\frac{1}{2}\mu_I + \mu_S| = m_K$ The coefficient of the order α^4 term can be shown to be positive when evaluated at $\frac{1}{2}\mu_I + \mu_S = m_K$. This shows there is a second-order transition to a kaon-condensed phase at $\frac{1}{2}\mu_I + \mu_S = \pm m_K$. For the transition to a neutral kaon-condensed phase, we have $-\frac{1}{2}\mu_I + \mu_S = \pm m_K$.

While the transitions from the vacuum to either a pion-condensed phase or a kaon-condensed phase are second order, the transition between the two Bose-condensed phases is first order. At leading, this is straightforward to see. For example the pion and kaon condensates are given by

$$\langle \pi^+ \rangle = 2f^2 B_0 \sin\alpha = 2f^2 B_0 \sqrt{1 - \frac{m_\pi^4}{\mu_I^4}}\,, \qquad \mu_I > m_\pi \tag{6.14}$$

$$\langle K^+ \rangle = 2f^2 B_0 \sin\alpha = 2f^2 B_0 \sqrt{1 - \frac{m_K^4}{(\frac{1}{2}\mu_I + \mu_S)^4}}\,, \qquad \frac{1}{2}\mu_I + \mu_S > m_K\,. \tag{6.15}$$

For any $\mu_I > m_\pi$ and $\frac{1}{2}\mu_I + \mu_S > m_K$, these condensates jump discontinuously to zero as we cross the phase line. The transition line itself is given by the equality of the pressures in the two phases. While it is possible to find this line analytically at tree level as shown in eq. (3.27), in order to find the line at NLO, we need to compare the pressure in the pion and kaon condensed phases, which can only be done numerically. We have performed this calculation for the central values from eqs. (6.4) and (6.6). In figure 2 we show the phase diagram in the μ_I–μ_S plane with the first order transition line increasing to higher strange chemical potential for all values of the isospin chemical potential greater than the pion mass. The vacuum phase is in the region bounded by the straight lines $\mu_I = \pm m_\pi$, $\mu_S = \pm(\frac{1}{2}\mu_I + m_K)$, and $\mu_S = \pm(-\frac{1}{2}\mu_I + m_K)$. The corners from where the first-order lines emerge are located at $(\mu_I, \mu_S) = (\pm 131, \pm 415.5)\,\text{MeV}$. The solid lines represent second-order transitions while the dashed line indicates the tree level first-order transition and the green dot dashed line indicates the NLO first-order transition. In the vacuum phase, the thermodynamic functions are independent of the isospin and strange chemical potentials. This is an example of the so-called Silver Blaze property [55].

6.2 Medium-dependent masses

In this subsection, we will briefly discuss the medium-dependent masses. We restrict ourselves to a leading-order calculation, i.e. we consider the tree-level dispersion relations evaluated at $p^2 = 0$. In the pion-condensed phase, they are given by eqs. (3.77)–(3.81). In the kaon-condensed phase, they are given by eqs. (3.100)–(3.104). In the left panel of figure 3, we show the medium-dependent masses as a function of the isospin chemical potential μ_I for fixed strange chemical potential $\mu_S = 200\,\text{MeV}$. For $\mu_I = 0$, we are in the normal phase, the pion masses take on their vacuum values, while the kaons are degenerate in pairs. The mass of π^+ decreases as we increase μ_I and vanishes when $\mu_I = m_\pi$ and enter the pion-condensed phase. At $\mu_I = m_\pi$, the masses vary continuously reflecting the second-order nature of the transition. We also note that the mass of η^0 is independent of μ_I. which follows directly from eq. (3.81). Finally, for asymptotically large values of μ_I,

JHEP06(2020)170

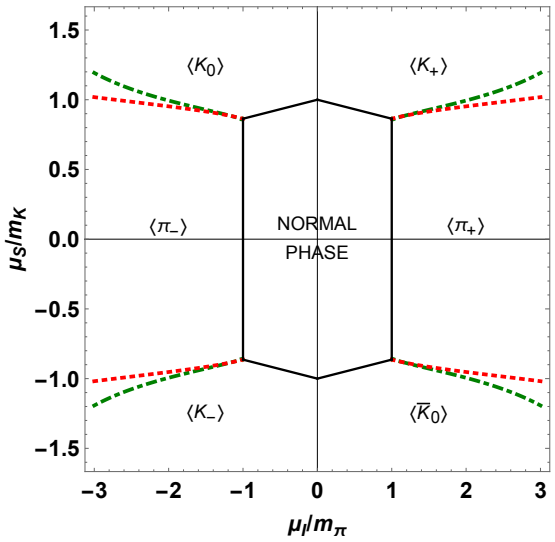

Figure 2. Phase diagram in the μ_I–μ_S plane at $T = 0$. Solid lines represent second-order transitions while the red dashed lines are the tree level first-order transitions and the green dot-dashed lines are the NLO first-order transitions. The normal phase has vanishing meson condensates and the meson condensate that becomes non-zero is indicated in each region.

the kaons and pions are pairwise degenerate. In the right panel of figure 3, we show the medium-dependent masses as a function of isospin chemical potential μ_I for fixed strange chemical potential $\mu_S = 460\,\text{MeV}$. At $\mu_I = 0$, we are in the vacuum phase. The kaons are again degenerate in pairs, the pions are also degenerate taking on their vacuum values. We enter the kaon-condensed phase at $\mu_I = 42\,\text{MeV}$, which is a second-order transition. In this phase, K^+ is the Goldstone mode associated with the spontaneous breakdown of the U(1)-symmetry. As we increase the isospin chemical potential past approximately $\mu_I = 268\,\text{MeV}$, we enter the pion-condensed phase. In this phase, π^+ is the Goldstone mode associated with the spontanous breakdown of the $\text{U}(1)_{I_3}$-symmetry. This first-order nature of the transition can be seen by the jumps in the quasiparticle masses.

Finally, we also note that in the charged pion and kaon condensed phases the mass eigenstates do not coincide with the charge eigenstates [56]. It is easy to see using the form of the inverse propagators in eqs. (3.62) and (3.84) that in the condensed phases the mass eigenstates can be found using momentum-dependent rotations of the mass eigenstates. However, the pion and kaon charge eigenstates are the standard ones

$$\pi^{\pm} = \frac{\phi_1 \mp i\phi_2}{\sqrt{2}}\,, \qquad K^{\pm} = \frac{\phi_4 \mp i\phi_5}{\sqrt{2}}\,. \tag{6.16}$$

They can be deduced using the canonical form of the quadratic, kinetic terms in eqs. (3.61) and (3.83) in the unbroken phase with $\alpha = 0$, which possesses a global U(1) symmetry. When gauged (using electromagnetic fields), the Lagrangian possesses a local U(1) (gauge) symmetry, which is broken by the pion condensed phase.

JHEP06(2020)170

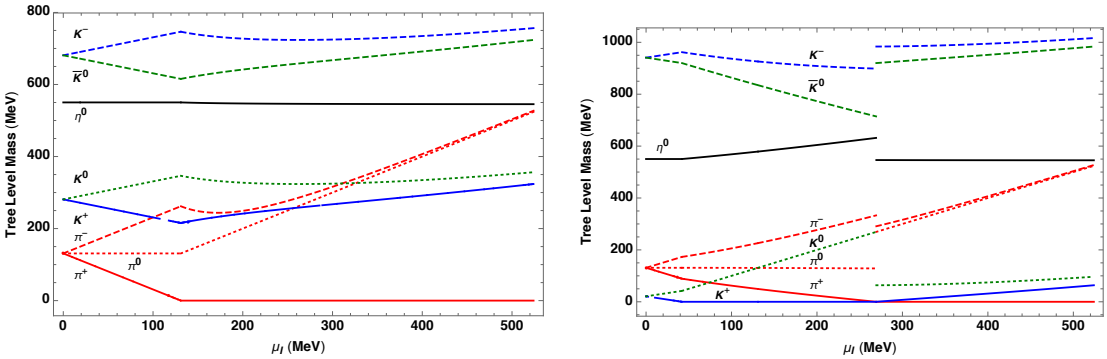

Figure 3. Medium-dependent masses as a function of μ_I for $\mu_S = 200\,\text{MeV}$ (left panel) and $\mu_S = 460\,\text{MeV}$ (right panel). See main text for details.

6.3 Pressure, isospin density, and equation of state

In this subsection, we discuss the pressure, the isospin density and the equation of state in the pion-condensed phase and compare our results to the $(2+1)$-flavor lattice QCD results of refs. [43–45]. We begin with figure 4, where we plot the pressure (divided by m_π^4) as a function of μ_I/m_π. The pressure has been normalized to be zero in the normal vacuum, which also has a zero isospin density. As pions condense beginning at the critical isospin chemical potential, $\mu_I^c = m_\pi$, the pressure increases with increasing chemical potential and continues to increase monotonically, a feature that is consistent with results from lattice QCD. The pressure from two-flavor χPT is smaller than that from lattice QCD even when the uncertainties within the LECs, the pion mass and pion decay constant are taken into account. The range of pressures due to the uncertainties calculated within two-flavor χPT is represented by the blue band. We find that the uncertainty in the pion mass and the pion decay constant (as opposed to the uncertainty in the LECs) dominates the uncertainty in the pressure. On the other hand, the pressure from three-flavor χPT (shown in green), which includes the contribution from strange quarks unlike two-flavor χPT, overestimates the pressure. In figure 4, we use a dark green band to show the uncertainty in the pressure due to the uncertainties in the pion mass and the pion decay constant, and we use a light green band to represents the uncertainty in the pressure due to the LECs, the pion mass and the pion decay constant. The result shows that unlike in two-flavor χPT, the uncertainty in the pressure is dominated by the uncertainty in the LECs.

It is clear from figure 4 that the difference in pressure calculated in two-flavor χPT versus that calculated in three-flavor χPT is quite significant. The tree level pressure in two and three-flavor χPT is identical. Therefore, the difference arises through the NLO contribution to the pressure in two-flavor and three-flavor χPT. Since the NLO contribution is suppressed by a power of $1/(4\pi f_\pi)^2$, the difference in the two-flavor and three-flavor pressure seems unusually large. In order to explain the difference we have mapped three-flavor χPT by expanding the effective potential in the limit of large strange quark masses in subsection 5.2. After identifying the appropriate two-flavor LECs in terms of three-flavor LECs — see eqs. (5.11)–(5.15) — we find the appropriate two-flavor LECs that are

JHEP06(2020)170

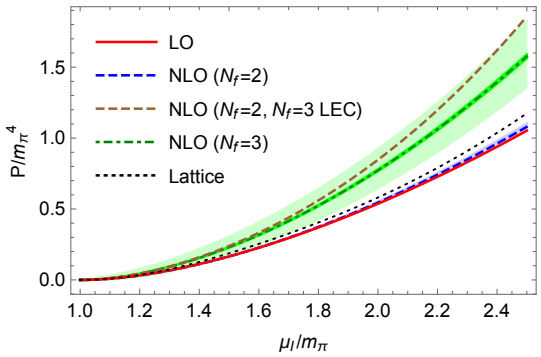

Figure 4. Normalized Pressure (P/m_π^4) as a function of μ_I/m_π at LO (red), at NLO with two flavors (blue), NLO with three flavors (green), and NLO with two flavors and three-flavor LECs (brown). See main text for details.

consistent with the values of three-flavor LECs. They are

$$\bar{l}_1(N_f=3)=14.5,\ \bar{l}_2(N_f=3)=6.5,\ \bar{l}_3(N_f=3)=4.1,\ \bar{l}_4(N_f=3)=4.2\,, \tag{6.17}$$

with $\bar{l}_i$ being defined in eq. (5.16). In order to contrast the above values with the two-flavor LECs, we state the LECs below where

$$\bar{l}_1(N_f=2)=-0.4,\ \bar{l}_2(N_f=2)=4.3,\ \bar{l}_3(N_f=2)=2.9,\ \bar{l}_4(N_f=2)=4.4\,. \tag{6.18}$$

We note that while $\bar{l}_4$ looks quite similar in the two cases, $\bar{l}_2$ and $\bar{l}_3$ are somewhat different with the difference in $\bar{l}_1$ being the most significant (they have opposite signs). We calculated the pressure in two-flavor χPT using the LECs found to be consistent with three-flavor χPT — we show this result in figure 4 in brown (dashed). The result shows that even the two-flavor χPT overestimates the pressure compared to that from 2+1 flavor lattice QCD. This analysis shows that the overestimation of the pressure is due to the values of the LECs of three-flavor χPT, which also have large uncertainties compared to two-flavor LECs. As a secondary observation, we note that as the strange quark mass becomes lighter, the pressure increases in χPT, particularly for larger isospin chemical potential.

In figure 5, we plot the isospin density (divided by m_π^3) as a function of the normalized chemical potential, μ_I/m_π. The isospin density is zero in the vacuum phase and monotonically increases in the pion-condensed phase. The rate of increase decreases as the isospin chemical potential increases. The isospin density from three-flavor χPT is consistent with that of lattice QCD in the normal vacuum and near the critical isospin chemical potential up to approximately $\mu_I = 1.4m_\pi$. For larger isospin chemical potentials, three-flavor χPT consistently overestimates the isospin density. This is unlike the result in two-flavor χPT which is in extremely good agreement with lattice QCD. The two-flavor χPT result using three-flavor LECs is plotted in brown and shows that the three-flavor χPT result is largely explained by the discrepancy in the values of the LECs in two-flavor and three-flavor χPT.

JHEP06(2020)170

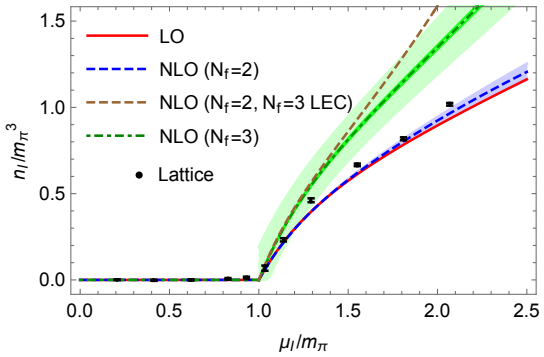

Figure 5. Normalized isospin density (n_I/m_π^3) as a function of μ_I/m_π at LO (red), at NLO with two flavors (blue), NLO with three flavors (green), and NLO with two flavors and three-flavor LECs (brown). See main text for details.

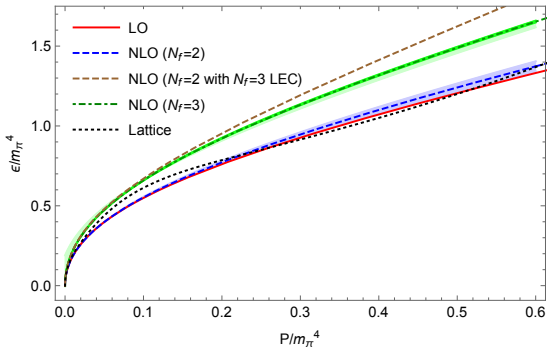

Figure 6. Normalized energy density (ϵ/μ_I^4) as a function of the normalized pressure (P/m_π^4) at NLO with two flavors (blue), NLO with three flavors (green), and NLO with two flavors and three-flavor LECs (brown). See main text for details.

Finally, in figure 6 we plot the equation of state: the energy density divided by m_π^4 is plotted against the pressure divided by m_π^4. Three-flavor χPT consistently overestimates the energy density for all pressures though up to $P/m_\pi^4 \simeq 0.10$, the discrepancy is small. Two-flavor χPT, on the other hand, underestimates the energy density up to $P/m_\pi^4 \approx 0.2$ but is largely consistent for values above it. Using three-flavor LECs, we can show that most of the discrepancy between two-flavor and three-flavor χPT is due to the discrepancy between the two sets of LECs, a theme common to all observables we have calculated in this work. The two-flavor results using three-flavor LEC is shown using brown dashed lines. The result is consistent with three-flavor χPT for $P/m_\pi^4 \simeq 0.2$ while above it the two-flavor χPT result gives larger values of energy density. It is also worth noting that for a given value of pressure the energy density decreases with decreasing strange quark masses.

JHEP06(2020)170

Acknowledgments

The authors would like to thank B. Brandt, G. Endrődi and S. Schmalzbauer for useful discussions as well as for providing the data points of ref. [7]. P.A. would like to acknowledge the hospitality of the Niels Bohr International Academy, where a portion of the work was done.

A Meson masses and decay constants

In order to show the second-order nature of the phase transition from the vacuum to a Bose-condensed phase at $\mu_I^c = m_\pi$, and $\pm\frac{1}{2}\mu_I^c + \mu_S^c = m_K$ where m_π and m_K are the physical meson masses in the vacuum, we need to express them in terms of the parameters $B_0 m$, $B_0 m_s$, and f of the chiral Lagrangian. The pion and kaon masses are [10]

$$m_\pi^2 = m_{\pi,0}^2 \left[1 - \left(8L_4^r + 8L_5^r - 16L_6^r - 16L_8^r + \frac{1}{2(4\pi)^2} \log \frac{\Lambda^2}{m_{\pi,0}^2} \right) \frac{m_{\pi,0}^2}{f^2} \right.$$
$$\left. - (L_4^r - 2L_6^r) \frac{16 m_{K,0}^2}{f^2} + \frac{m_{\eta,0}^2}{6(4\pi)^2 f^2} \log \frac{\Lambda^2}{m_{\eta,0}^2} \right] , \tag{A.1}$$

$$m_K^2 = m_{K,0}^2 \left[1 - (L_4^r - 2L_6^r) \frac{8 m_{\pi,0}^2}{f^2} - (2L_4^r + L_5^r - 4L_6^r - 2L_8^r) \frac{8 m_{K,0}^2}{f^2} \right.$$
$$\left. - \frac{m_{\eta,0}^2}{3(4\pi)^2 f^2} \log \frac{\Lambda^2}{m_{\eta,0}^2} \right] . \tag{A.2}$$

The pion and kaon decay constants, f_π and f_K respectively, are [10]

$$f_\pi^2 = f^2 \left[1 + \left(8L_4^r + 8L_5^r + \frac{2}{(4\pi)^2} \log \frac{\Lambda^2}{m_{\pi,0}^2} \right) \frac{m_{\pi,0}^2}{f^2} \right.$$
$$\left. + \left(16L_4^r + \frac{1}{(4\pi)^2} \log \frac{\Lambda^2}{m_{K,0}^2} \right) \frac{m_{K,0}^2}{f^2} \right] \tag{A.3}$$

$$f_K^2 = f^2 \left[1 + \left(12L_4^r + \frac{3}{4(4\pi)^2} \log \frac{\Lambda^2}{m_{\pi,0}^2} \right) \frac{m_{\pi,0}^2}{f^2} + \left(8L_5^r + \frac{3}{2(4\pi)^2} \log \frac{\Lambda^2}{m_{K,0}^2} \right) \frac{m_{K,0}^2}{f^2} \right.$$
$$\left. + \left(12L_4^r + \frac{3}{4(4\pi)^2} \log \frac{\Lambda^2}{m_{\eta,0}^2} \right) \frac{m_{\eta,0}^2}{f^2} \right] . \tag{A.4}$$

Using the expressions for the renormalization group equations, eq. (2.16), it is straightforward to see that the Λ-dependence of the coupling cancels against the chiral logarithms in expressions for the masses and decay constants.

JHEP06(2020)170

References

[1] K. Fukushima and T. Hatsuda, *The phase diagram of dense QCD*, *Rept. Prog. Phys.* **74** (2011) 014001 [arXiv:1005.4814] [INSPIRE].

[2] S. Hands, I. Montvay, S. Morrison, M. Oevers, L. Scorzato and J.-I. Skullerud, *Numerical study of dense adjoint matter in two color QCD*, *Eur. Phys. J.* **C 17** (2000) 285 [hep-lat/0006018] [INSPIRE].

[3] K. Rajagopal and F. Wilczek, *The condensed matter physics of QCD*, in *At the frontier of particle physics*, volume 3, World Scientific, Singapore (2001), pg. 2061.

[4] M.G. Alford, A. Schmitt, K. Rajagopal and T. Schäfer, *Color superconductivity in dense quark matter*, *Rev. Mod. Phys.* **80** (2008) 1455 [arXiv:0709.4635] [INSPIRE].

[5] S. Carignano, L. Lepori, A. Mammarella, M. Mannarelli and G. Pagliaroli, *Scrutinizing the pion condensed phase*, *Eur. Phys. J.* **A 53** (2017) 35 [arXiv:1610.06097] [INSPIRE].

[6] H. Abuki, T. Brauner and H.J. Warringa, *Pion condensation in a dense neutrino gas*, *Eur. Phys. J.* **C 64** (2009) 123 [arXiv:0901.2477] [INSPIRE].

[7] B.B. Brandt et al., *New class of compact stars: pion stars*, *Phys. Rev.* **D 98** (2018) 094510 [arXiv:1802.06685] [INSPIRE].

[8] S. Weinberg, *Phenomenological Lagrangians*, *Physica* **A 96** (1979) 327 [INSPIRE].

[9] J. Gasser and H. Leutwyler, *Chiral perturbation theory to one loop*, *Annals Phys.* **158** (1984) 142 [INSPIRE].

[10] J. Gasser and H. Leutwyler, *Chiral perturbation theory: expansions in the mass of the strange quark*, *Nucl. Phys.* **B 250** (1985) 465 [INSPIRE].

[11] J. Bijnens, G. Colangelo and G. Ecker, *Renormalization of chiral perturbation theory to order p^6*, *Annals Phys.* **280** (2000) 100 [hep-ph/9907333] [INSPIRE].

[12] S. Scherer, *Introduction to chiral perturbation theory*, *Adv. Nucl. Phys.* **27** (2003) 277 [hep-ph/0210398] [INSPIRE].

[13] D.T. Son and M.A. Stephanov, *QCD at finite isospin density: from pion to quark-anti-quark condensation*, *Phys. Atom. Nucl.* **64** (2001) 834 [hep-ph/0011365] [INSPIRE].

[14] M. Loewe and C. Villavicencio, *Thermal pions at finite isospin chemical potential*, *Phys. Rev.* **D 67** (2003) 074034 [hep-ph/0212275] [INSPIRE].

[15] E.S. Fraga, L.F. Palhares and C. Villavicencio, *Quark mass and isospin dependence of the deconfining critical temperature*, *Phys. Rev.* **D 79** (2009) 014021 [arXiv:0810.1060] [INSPIRE].

[16] T.D. Cohen and S. Sen, *Deconfinement transition at high isospin chemical potential and low temperature*, *Nucl. Phys.* **A 942** (2015) 39 [arXiv:1503.00006] [INSPIRE].

[17] O. Janssen, M. Kieburg, K. Splittorff, J.J.M. Verbaarschot and S. Zafeiropoulos, *Phase diagram of dynamical twisted mass Wilson fermions at finite isospin chemical potential*, *Phys. Rev.* **D 93** (2016) 094502 [arXiv:1509.02760] [INSPIRE].

[18] S. Carignano, A. Mammarella and M. Mannarelli, *Equation of state of imbalanced cold matter from chiral perturbation theory*, *Phys. Rev.* **D 93** (2016) 051503 [arXiv:1602.01317] [INSPIRE].

JHEP06(2020)170

[19] L. Lepori and M. Mannarelli, *Multicomponent meson superfluids in chiral perturbation theory*, *Phys. Rev.* **D 99** (2019) 096011 [arXiv:1901.07488] [INSPIRE].

[20] S. Cotter, P. Giudice, S. Hands and J.-I. Skullerud, *Towards the phase diagram of dense two-color matter*, *Phys. Rev.* **D 87** (2013) 034507 [arXiv:1210.4496] [INSPIRE].

[21] K. Splittorff, D.T. Son and M.A. Stephanov, *QCD-like theories at finite baryon and isospin density*, *Phys. Rev.* **D 64** (2001) 016003 [hep-ph/0012274] [INSPIRE].

[22] D. Toublan and J.B. Kogut, *Isospin chemical potential and the QCD phase diagram at nonzero temperature and baryon chemical potential*, *Phys. Lett.* **B 564** (2003) 212 [hep-ph/0301183] [INSPIRE].

[23] L. He and P.-F. Zhuang, *Phase structure of Nambu-Jona-Lasinio model at finite isospin density*, *Phys. Lett.* **B 615** (2005) 93 [hep-ph/0501024] [INSPIRE].

[24] L.-Y. He, M. Jin and P.-F. Zhuang, *Pion superfluidity and meson properties at finite isospin density*, *Phys. Rev.* **D 71** (2005) 116001 [hep-ph/0503272] [INSPIRE].

[25] L. He, M. Jin and P.-F. Zhuang, *Pion condensation in baryonic matter: from sarma phase to Larkin-Ovchinnikov-Fudde-Ferrell phase*, *Phys. Rev.* **D 74** (2006) 036005 [hep-ph/0604224] [INSPIRE].

[26] D. Ebert and K.G. Klimenko, *Gapless pion condensation in quark matter with finite baryon density*, *J. Phys.* **G 32** (2006) 599 [hep-ph/0507007] [INSPIRE].

[27] D. Ebert and K.G. Klimenko, *Pion condensation in electrically neutral cold matter with finite baryon density*, *Eur. Phys. J.* **C 46** (2006) 771 [hep-ph/0510222] [INSPIRE].

[28] G.-F. Sun, L. He and P.-F. Zhuang, *BEC-BCS crossover in the Nambu-Jona-Lasinio model of QCD*, *Phys. Rev.* **D 75** (2007) 096004 [hep-ph/0703159] [INSPIRE].

[29] J.O. Andersen and L. Kyllingstad, *Pion condensation in a two-flavor NJLS model: the role of charge neutrality*, *J. Phys.* **G 37** (2009) 015003 [hep-ph/0701033] [INSPIRE].

[30] H. Abuki, R. Anglani, R. Gatto, M. Pellicoro and M. Ruggieri, *The fate of pion condensation in quark matter: from the chiral to the real world*, *Phys. Rev.* **D 79** (2009) 034032 [arXiv:0809.2658] [INSPIRE].

[31] C.-F. Mu, L.-Y. He and Y.-X. Liu, *Evaluating the phase diagram at finite isospin and baryon chemical potentials in the Nambu-Jona-Lasinio model*, *Phys. Rev.* **D 82** (2010) 056006 [INSPIRE].

[32] T. Xia, L. He and P. Zhuang, *Three-flavor Nambu-Jona-Lasinio model at finite isospin chemical potential*, *Phys. Rev.* **D 88** (2013) 056013 [arXiv:1307.4622] [INSPIRE].

[33] S.S. Avancini, A. Bandyopadhyay, D.C. Duarte and R.L.S. Farias, *Cold QCD at finite isospin density: confronting effective models with recent lattice data*, *Phys. Rev.* **D 100** (2019) 116002 [arXiv:1907.09880] [INSPIRE].

[34] Z.-Y. Lu, C.-J. Xia and M. Ruggieri, *Thermodynamics and susceptibilities of isospin imbalanced QCD matter*, *Eur. Phys. J.* **C 80** (2020) 46 [arXiv:1907.11497] [INSPIRE].

[35] K. Kamikado, N. Strodthoff, L. von Smekal and J. Wambach, *Fluctuations in the quark-meson model for QCD with isospin chemical potential*, *Phys. Lett.* **B 718** (2013) 1044 [arXiv:1207.0400] [INSPIRE].

JHEP06(2020)170

[36] H. Ueda, T.Z. Nakano, A. Ohnishi, M. Ruggieri and K. Sumiyoshi, *QCD phase diagram at finite baryon and isospin chemical potentials in Polyakov loop extended quark meson model with vector interaction*, *Phys. Rev.* **D 88** (2013) 074006 [arXiv:1304.4331] [INSPIRE].

[37] R. Stiele, E.S. Fraga and J. Schaffner-Bielich, *Thermodynamics of $(2+1)$-flavor strongly interacting matter at nonzero isospin*, *Phys. Lett.* **B 729** (2014) 72 [arXiv:1307.2851] [INSPIRE].

[38] P. Adhikari, J.O. Andersen and P. Kneschke, *Pion condensation and phase diagram in the Polyakov-loop quark-meson model*, *Phys. Rev.* **D 98** (2018) 074016 [arXiv:1805.08599] [INSPIRE].

[39] G. Endrődi, *Magnetic structure of isospin-asymmetric QCD matter in neutron stars*, *Phys. Rev.* **D 90** (2014) 094501 [arXiv:1407.1216] [INSPIRE].

[40] P. Adhikari, *Magnetic vortex lattices in finite isospin chiral perturbation theory*, *Phys. Lett.* **B 790** (2019) 211 [arXiv:1810.03663] [INSPIRE].

[41] J.B. Kogut and D.K. Sinclair, *Quenched lattice QCD at finite isospin density and related theories*, *Phys. Rev.* **D 66** (2002) 014508 [hep-lat/0201017] [INSPIRE].

[42] J.B. Kogut and D.K. Sinclair, *Lattice QCD at finite isospin density at zero and finite temperature*, *Phys. Rev.* **D 66** (2002) 034505 [hep-lat/0202028] [INSPIRE].

[43] B.B. Brandt and G. Endrődi, *QCD phase diagram with isospin chemical potential*, PoS(LATTICE2016)039 (2016) [arXiv:1611.06758] [INSPIRE].

[44] B.B. Brandt, G. Endrődi and S. Schmalzbauer, *QCD at finite isospin chemical potential*, *EPJ Web Conf.* **175** (2018) 07020 [arXiv:1709.10487] [INSPIRE].

[45] B.B. Brandt, G. Endrődi and S. Schmalzbauer, *QCD phase diagram for nonzero isospin-asymmetry*, *Phys. Rev.* **D 97** (2018) 054514 [arXiv:1712.08190] [INSPIRE].

[46] M. Mannarelli, *Meson condensation*, *Particles* **2** (2019) 411 [arXiv:1908.02042] [INSPIRE].

[47] J.B. Kogut and D. Toublan, *QCD at small nonzero quark chemical potentials*, *Phys. Rev.* **D 64** (2001) 034007 [hep-ph/0103271] [INSPIRE].

[48] P. Adhikari, J.O. Andersen and P. Kneschke, *Two-flavor chiral perturbation theory at nonzero isospin: pion condensation at zero temperature*, *Eur. Phys. J.* **C 79** (2019) 874 [arXiv:1904.03887] [INSPIRE].

[49] P. Adhikari and J.O. Andersen, *QCD at finite isospin density: chiral perturbation theory confronts lattice data*, *Phys. Lett.* **B 804** (2020) 135352 [arXiv:1909.01131] [INSPIRE].

[50] M. Frank, M. Buballa and M. Oertel, *Flavor mixing effects on the QCD phase diagram at nonvanishing isospin chemical potential: one or two phase transitions?*, *Phys. Lett.* **B 562** (2003) 221 [hep-ph/0303109] [INSPIRE].

[51] A. Barducci, R. Casalbuoni, G. Pettini and L. Ravagli, *A calculation of the QCD phase diagram at finite temperature and baryon and isospin chemical potentials*, *Phys. Rev.* **D 69** (2004) 096004 [hep-ph/0402104] [INSPIRE].

[52] G. Colangelo, J. Gasser and H. Leutwyler, *$\pi\pi$ scattering*, *Nucl. Phys.* **B 603** (2001) 125 [hep-ph/0103088] [INSPIRE].

[53] K. Splittorff, D. Toublan and J.J.M. Verbaarschot, *Diquark condensate in QCD with two colors at next-to-leading order*, *Nucl. Phys.* **B 620** (2002) 290 [hep-ph/0108040] [INSPIRE].

JHEP06(2020)170

[54] K. Splittorff, D. Toublan and J.J.M. Verbaarschot, *Thermodynamics of chiral symmetry at low densities*, *Nucl. Phys.* **B 639** (2002) 524 [hep-ph/0204076] [INSPIRE].

[55] T.D. Cohen, *Functional integrals for QCD at nonzero chemical potential and zero density*, *Phys. Rev. Lett.* **91** (2003) 222001 [hep-ph/0307089] [INSPIRE].

[56] A. Mammarella and M. Mannarelli, *Intriguing aspects of meson condensation*, *Phys. Rev.* **D 92** (2015) 085025 [arXiv:1507.02934] [INSPIRE].

[57] B.B. Brandt and G. Endrődi, *Reliability of Taylor expansions in QCD*, *Phys. Rev.* **D 99** (2019) 014518 [arXiv:1810.11045] [INSPIRE].

[58] G. Endrődi, private communication.

[59] J. Bijnens and G. Ecker, *Mesonic low-energy constants*, *Ann. Rev. Nucl. Part. Sci.* **64** (2014) 149 [arXiv:1405.6488] [INSPIRE].

[60] B. Ananthanarayan, J. Bijnens and S. Ghosh, *An analytic analysis of the pion decay constant in three-flavoured chiral perturbation theory*, *Eur. Phys. J.* **C 77** (2017) 497 [arXiv:1703.00141] [INSPIRE].

JHEP06(2020)170